

Modeling of the Brain for Injury Prevention

King H. Yang, Haojie Mao, Christina Wagner, Feng Zhu, Clifford C. Chou and Albert I. King

Abstract From an ethical point of view, it is extremely difficult to propose a well-controlled human subject study aimed at understanding brain injury mechanisms and establishing the associated tolerance values. For this reason, many numerical models of the human and animal head or brain have been developed over the past several decades in an attempt to obtain in-depth insights into brain injury biomechanics, minimizing the need for human subject research. This chapter highlights and contrasts the essence of human and animal head numerical models developed for studying blunt impact and blast-induced brain injuries. Even with the vast amount of literature produced by these investigations and studies, the precise mechanisms of brain injury have not yet been fully established to date.

Through this review, it is clear that a lot of information can be garnered by numerical brain modeling but few efforts have been devoted so far to using these numerical models to provide guidelines in the discovery of brain injury mechanisms. Based on the brain models reported in the current literature, there are some inherent deficiencies. However, with further revisions and improvements to the currently available models, as opposed to developing new models from scratch, these issues can be overcome, and the state of the art can be advanced. More research effort into brain injury mechanisms, especially under in vivo conditions, is needed for computational model improvements so that the injury mechanisms can be thoroughly understood and effective countermeasures for protecting human from traumatic brain injury can be developed.

K. H. Yang (✉) · H. Mao · C. Wagner · F. Zhu · C. C. Chou · A. I. King
Wayne State University, Detroit, USA
e-mail: aa0007@wayne.edu; di8797@wayne.edu

1 Introduction

Traumatic brain injury (TBI) resulting from vehicular collisions, contact sports, falls, or blasts can have devastating consequences. Brain injuries not only pose a serious disability for those involved, but also place an enormous burden on society, often exacting a heavy economical, social, and emotional price. To reduce the likelihood and effects of these injuries, impact biomechanics, also referred to as the science of injury control, has been established as the field which aims to protect humans through the application of established engineering and medical research methods. The four general areas in the field of impact biomechanics involve the study of injury mechanisms, mechanical response to impact, injury tolerance, and assessment of the effectiveness of countermeasures using human surrogates. Although numerous research projects have been conducted, established scientific knowledge in all four areas of head impact biomechanics remains limited and an important area of modern research.

Modern day impact biomechanics research can be traced back to 1939 when Professor H. R. Lissner (a professor in Engineering) and Dr. E. S. Gurdjian (a neurosurgeon) began studying the mechanism of skull fracture at Wayne State University (WSU). They placed human skulls at the bottom of an elevator shaft and dropped steel balls onto these specimens from as high as the 12th floor. Since then, numerous investigations have been conducted to further our understanding of injury mechanisms, impact response, and injury tolerance. Experimental studies include the use of animals, physical models, volunteers, and cadavers and have subsequently led to the companion development of mathematical and computational models to enhance the understanding of brain injury. These virtual models can allow for more in-depth biomechanics studies, if properly developed and validated.

Based on globally measured parameters in these studies, numerous textbooks and articles affirmed that brain injury is due to one or more of the following mechanisms: (1) positive pressure, (2) negative pressure, (3) pressure gradient, and/or (4) rotational effects. Positive pressure, typically associated with the so-called coup injury mechanism, is assumed to be the result of the moving skull towards the stationary brain, producing a compressive wave in the brain at the time of impact or direct compression of the brain due to in-bending of the skull. Negative pressure, which has been associated with the so-called contrecoup injury mechanism, is hypothesized to be the result of tension generated by skull moving away from the brain that is lagging behind skull. Alternately, the negative pressure could be due to a tensile wave that was formed by the reflection of the original compression wave off the skull. Cavitation (collapse of a vapor bubble) occurs if negative pressure is lower than the vapor pressure of water and may also damage brain tissues. Additionally, shear stresses resulting from high pressure gradients in areas such as junctions between gray matter and white matter have been associated with diffuse axonal injury (DAI), but despite this, no techniques have been developed to physically measure intracranial shear stress experimentally. This shear mechanism has been postulated to explain why massive loss of neuronal

function is seen in the central areas of the brain in some injuries. Lastly, rotational acceleration or velocity has been associated with several types of brain injury, such as surface contusions due to frictional contact of the smooth brain on the rough bony cranial vault, pulling of the brainstem through the foramen magnum, acute subdural hematoma (ASDH) as a result of ruptured bridging veins due to large relative motion between the brain and skull, and concussion or DAI due to high shear deformation of the brain owing to the high bulk modulus with low shear modulus. The reader is cautioned that not all hypothesized statements made above have been scientifically validated or proven. In particular, the shearing of axons is difficult to imagine considering that it is not a very stiff material. Also, it can be shown from first principles of fluid mechanics that rupture of the bridging vein is not the cause of ASDH. This highlights why further research in TBI is necessary.

In addition to blunt injury mechanisms, recent conflicts in the Middle East have ignited a debate regarding blast wave induced TBI. As early as the 1950s, Gurdjian and colleagues observed that direct impacts to the head could generate pressure waves in the brain. They performed the first fluid percussion experiment on dogs to recreate this phenomenon. Without any global head acceleration, brain injuries were observed, although it remains uncertain as to whether these injuries included DAI or not. In any case, this mechanism was “forgotten” for some time and is being rekindled due to the many mild TBI injuries attributed to blast overpressure in which global head motion may not be occurring.

To research these and other brain injury mechanisms, experimental animal models are used as human surrogates to provide an opportunity to monitor the brain’s physiologic response over time, which can rarely be done in human studies. However, methods for extrapolating or scaling animal biomechanical data or tolerances to the human are often unreliable, and some researchers have raised ethical concerns on the use of animal subjects. As an alternative, physical models may provide good control over the experimental setup but the mechanism of injury cannot be delineated from such models due, in part, to poor biofidelity. Data from volunteers, which removes biofidelity issues, are very sparse, and experiments can only be performed under uncontrolled conditions (such as real world athletic events) or under controlled conditions in a laboratory at impact severities well below the injury level. Although human cadavers allow for well-controlled tests and have the same anatomical features as a living person, the lack of muscular and physiological responses limits the scientist’s ability to assess acute as well as secondary sequelae. That is to say, pathophysiological responses of the brain that are vital to the understanding of functional brain injury cannot be fully assessed. The ideal surrogate for brain injury research has yet to be discovered.

Possible surrogate candidates can be found in numerical modeling techniques, some of which have been in development for decades. Mathematical modeling of the head is a powerful tool for the study of head injury and associated head impact protection. In early models, simplified intracranial pressures and stresses in the skull were calculated based on lumped-mass-spring-damper models consisting of only a handful of degrees-of-freedom (e.g. [3, 31, 50, 51, 90, 131]). There were also models of fluid filled shells, mathematically represented by a set of partial

differential equations that were solved using either the infinite series method (e.g. [17, 29]) or the finite difference method (e.g. [91]). Readers are referred to the review article by King and Chou [66] for more detail on these early numerical models. In recent years, technological advances have allowed for the development of complex finite element (FE) head models, which mimic the irregular geometry and anatomical features of the head, with more than 1 million degrees-of-freedom (DOFs). Such computational models have been used to study brain impact response, mimicking the complex boundary and loading conditions. Simulated tissue level stress, strain and/or deformation distributions for a given biomechanical input, such as a direct impact or a non-impact inertial loading, are available for correlation with data obtained experimentally or from real-world incidents to establish injury mechanisms and thresholds. Based on the promise of these techniques, numerous FE head/brain models have been developed all over the world, but it is important to note that not every computational model will yield the same biomechanical conclusions, an issue that will be discussed further in concluding this review.

In this chapter, human and animal head FE models developed over the past several decades are reviewed and several directions for future research are highlighted. Due to length limitations, computational models developed for purposes other than injury research, such as those for studying brain-electromagnetic (EM) field interaction phenomena (e.g. [18]), neurosurgical procedures (e.g. Wittek et al. [154] on needle insertion into the brain; Saberi et al. [124] on effect of hematoma; Gao et al. [40] on decompressive effect of craniotomy; Hagemann et al. [44], Soza et al. [132] Gao et al. [39], Wittek et al. [153], Hu et al. [55], Chakrabarty and Hanson [15], on brain shift calculation), hematoma size and shape (e.g. [136]) are not included in this review. This review is divided into four major: [Sects. 2.1](#), [10.1](#), [10.2](#), and [10.3](#).

2 Literature Review

2.1 *Blunt Impact Brain Models*

Blunt impact induced TBI has caused significant numbers of death and disability among children and young adults in the United States [139]. It is estimated that 1.5 million Americans sustain a TBI annually, and 50,000 die each year from these injuries. Among the affected, 80,000 to 90,000 patients suffer permanent disability from their injuries [79]. In addition to being a major public health problem, TBI is also a major socioeconomic problem. The direct medical costs and indirect costs (such as lost productivity) of TBI totaled an estimated \$60 billion in the United States in 2000 [33]. As discussed previously, there are limited methods that can be used to study the mechanism of injury and evaluation of appropriate countermeasures. Computational models of the head have been and continue to be used to assist in this research.

The basic principle behind the FE method is that any structural system can be subdivided into a finite number of discrete elements and its response to loading approximated using nodal interconnections. Mechanical properties, such as elastic modulus, density, Poisson's ratio, and tangent modulus are assigned to each element to govern the material behavior. The geometric information and material properties for each element are used to form an element stiffness matrix. Static or dynamic structural deformations can then be calculated through the assembly of all element stiffness matrices, definition of appropriate boundary conditions, and application of loading conditions using physical energy conservation laws and differential equations. Therefore, this is a numerical method that is limited by computational resources and underlying approximations.

3 History of FE Head Modeling

Early FE models of the head generally assumed a simplified geometry due to the lack of computational power needed to solve the equations mentioned above. To the best of the authors' knowledge, the first three-dimensional (3D) FE head model with actual skull geometry was reported by Hardy and Marcal [45]. This model was used to simulate static frontal and lateral loading, although the model did not include representation of the brain. Chan [16] reported an axi-symmetric model with the skull and brain represented by viscoelastic materials and used the model to investigate the hypothesis that large shear stress could rupture the cerebral blood vessels and injure brain matter. Other earlier models used simplified spherical, spheroidal, or ellipsoidal shells to represent the skull and inviscid fluid, viscoelastic, or elastic materials to form the intracranial contents (e.g. [62, 63]).

A more realistic 3D FE model developed by Shugar [130] followed. In this model, the skull and brain were assumed to be linearly elastic, and the skull was represented by a layered structure to incorporate the inner and outer tables. This model was later refined by Ruan et al. [117] and Zhou et al. [163] with changes in material properties and the differentiation of gray and white matter in the brain model, discussed in the following subsections. Concurrently with Shugar's paper, Ward and colleagues at the Naval Construction Battalion Center and University of California at San Diego developed 3D human half-brain models which included the cerebrum, cerebellum, brainstem, ventricles, dural membrane, and a rigid skull [145, 147, 148] for studying frontal impacts. Compared to the Shugar model, this model was much more thoroughly validated. In the publication by Ward and Thompson [148], roller-supported linear springs were used to simulate the tethering of the brain to the skull, and the model was validated against data obtained from static measurements of the brainstem during flexion and extension of the head, as well as experimentally determined mode shapes and natural frequencies. The model was also validated against intracranial pressure time history data from a single test reported by Nahum et al. [97]. Based on results from these simulations, the authors noted that a model without the falx cerebri and tentorium could not

predict the superior brainstem deflections correctly. This conclusion has been echoed by a newer 2D model developed by Li et al. [82] at the Medical College of Wisconsin with the aim of evaluating the effect of falx with the head subjected to lateral impact. It is worth noting that the FE model reported by Hosey and Liu [54] used the same brain geometry as Ward and Thompson [148] and was reasonably complete, but was too large to be run on the computers available at that time, underscoring the difficulties in FE model development in the early history of the field. Utilizing animal and human studies, Ward et al. [147] further developed monkey and baboon brain models for calculating the differences in intracranial responses among animals and humans subjected to the same loading conditions. In 1979, Nahum et al. continued to investigate closed head injury and studied the effectiveness of helmets on protecting the brain [98]. In 1982, Ward reported that the predicted cortical displacement by their model under dynamic loading was too high [145]. Restraint conditions were added to the brain–skull interface and the Young’s modulus selected to represent the brain was increased to ten times that used in Ward’s study in order to lower the cortical displacement.

Eventually, Nahum et al. [99] expanded the half-brain model developed by Ward and Thompson [148] to a whole brain model, which was then used to predict subdural pressure under lateral impacts. Tests conducted by Nahum et al. [100] yielded multiple impact events along the lateral direction on one pressurized cadaver, with or without a helmet, and provided head linear and angular accelerations along with corresponding subdural pressures. The FE model simulations revealed a less distinct pressure gradient pattern than that seen in frontal impacts, and the authors suggested that this difference was due to the combination of all three components of linear acceleration not seen in frontal impacts. The authors also reported that the falx and tentorium played a significant role in compartmentalizing brain motion within each compartment, yet again accenting the importance of anatomical complexity in biomechanical models.

Besides the consequence of anatomy, these early head models also generated some insight into tissue material representation. In 1982, based on past experiences in brain modeling, Ward concluded that the brain should not be modeled as an incompressible material. A selective reduced integration scheme was suggested [145]. Specifically, a reduced integration scheme was used for the dilatational (volumetric) component, whereas a full integration scheme for the distortional (shear) component was used in conjunction with a nearly incompressible material representing the brain. The findings were summarized as follows: (a) brain models could accurately predict brain stresses or displacements if the model included the dural folds, falx, tentorium, foramen magnum, and effective compressibility, (b) stresses and strains developed in the brain lagged those in the skull, (c) coup and contrecoup contusions were caused by pressure associated with translational acceleration, (d) subdural hematomas were caused by high shear strains, (e) the occurrence and duration of concussion were related to the magnitude of the brain response, and (f) the largest shear strains were predicted along the brain–skull interface, brainstem, and cerebellum. It is suggested that readers should refer to a report by Khalil and Viano [64] for a discussion of the differences, similarities,

and the deficiencies of the FE models developed by the two groups led by Shugar and Ward.

Very few FE models were developed to study head and brain injury in the late-1970s or 1980s. One of few examples showing the use of FE models to investigate injury countermeasures, Saczalski et al. [125] developed a spherical brain model covered with a linear elastic dura, a linear elastic spherical skull, and a nonlinear scalp. The model-predicted pressure response was first qualitatively correlated with experimentally measured results before a helmet model was added to determine the effect of different liners. Despite the dearth of literature publications from this time, significant advancement on computational power, commercially available nonlinear finite element codes, meshing software, and graphical and animation tools became available during this period, indirectly facilitating the development of more complex numerical models of head and brain injuries. Since the 1990s, numerous FE head models have been developed around the globe for blunt impact analyses, and some iteration of many are still in use today. In the following subsections, these models are reviewed in accordance with the institutions where the model was first developed. As each institution developed their model independently, it is difficult to draw comparisons based on model predictions. Instead, one can assume it is more relevant to critique how the models were developed and how their predictions compare to experimentally measured data. It should be noted that tolerance values should not be compared between models, as these data are model-dependent, although trends can be seen throughout the brain modeling field.

4 Wayne State University

To investigate the dynamic response of the brain during side impact, Ruan et al. [117] developed an axi-symmetric model and two plane strain head models, which were subjected to a triangular pulse loading with a peak pressure of 40 kPa to determine the effects of mechanical properties of the skull, brain, and membrane. As these were 2D models, future refinements were made by the same authors to incorporate the geometry of the 3D FE head model reported by Shugar [130] to include most essential components of the head including the scalp, a three-layered skull, cerebrospinal fluid (CSF), dura mater, falx cerebri, and brain [118, 119]. The model-predicted time histories of the impact force, head acceleration, and intracranial pressure compared favorably with data from a single cadaveric subject reported by Nahum et al. [97]. Although one set of experimental data is obviously insufficient to validate a FE model, this was the only dataset reported by the authors in which time histories of the intracranial pressure were provided as opposed to peak pressures. For direct impact, a correlation was found between the head injury criterion (HIC) and intracranial pressure, and head acceleration and intracranial pressure. Biomechanical responses to varying impact locations (side, occipital and vertex), changes in impact velocity, and mass of the impactor were

studied parametrically using the model. A higher contrecoup pressure was predicted from an occipital impact than from a frontal impact. This finding supports clinical findings of contrecoup injury being more likely to result from an occipital impact than from a frontal impact. It was also reported that the maximum shear stress occurred in the brainstem.

The mesh of this model was refined and inhomogeneous material properties of the gray and white matter were added by Zhou et al. [163]. Additionally, ventricles and ten pairs of parasagittal bridging veins were incorporated into the model in an attempt to predict subdural hematoma when stretching of these veins exceeded their experimentally-determined tolerance limit. By prescribing different material properties of the gray and white matters, the authors found larger variations in the shear stress distribution patterns, without affecting the intracranial pressure, compared to the model with homogeneous properties. This finding is qualitatively similar to porcine experimental results in which diffuse axonal injuries were found in the white matter at its boundary with gray matter and near the ventricles [112] and underscores tissue differentiation as having a possible role in brain injury.

This model was coupled to a multilink rigid body model of the Hybrid III dummy, which is an anthropomorphic representation of the 50th percentile human male, to simulate human head responses during automotive barrier crashes [121]. Skull–isostress and brain–isostrain response curves were established based on these kinematics. The head model was further refined and exercised by Al-Bsharat et al. [2] through validation against intracranial pressure time histories reported by Nahum et al. [97]. While Nahum et al. [97] did not report time history curves for more than one test, they did report the peak pressure values for other test conditions although one of the peak values appeared to be an outlier. After excluding that data point, Al-Bsharat et al. were able to match their model predictions against all the other data points. Unfortunately, the relative displacements between the brain and the skull were far below the measured data reported by King et al. [67] using a high-speed X-ray system. To overcome this discrepancy, Al-Bsharat et al. [2] studied various types of numerical definition of the sliding interface between the brain and skull to determine the best scheme to represent the movement of the cerebral spinal fluid (CSF) layer. It was found that by adding a sliding interface between the brain and skull—more specifically, the interface between the pia and the arachnoid—model predictions of brain motion were found to match the measured displacements better.

With this improved model, Zhang et al. [160] investigated differences in brain response due to frontal and lateral impacts under identical impact and boundary conditions. Simulation results suggested that skull deformation and internal partitions of the brain may be responsible for the directional sensitivity of the head in terms of intracranial pressure and shear stress response. This conclusion is qualitatively consistent with experimental findings using subhuman primates in which a lateral impact was more injurious than a frontal impact of the same severity. Zhang et al. [160] also found that this version of the head model was numerically unstable when simulating large rotational impact.

To resolve this issue, a much more refined FE head model consisting almost eight times the number of elements was developed by Zhang et al. [161]. The new model had an anatomically detailed facial structure and used tri-linear solid elements and bi-linear membrane/shell elements to ensure numerical stability. Results indicated that this new model could be used to simulate direct and indirect impacts with combined translational and rotational accelerations as high as 200 g and 12,000 rad/s² or higher [161]. The model, referred to as the Wayne State University Head Injury Model (WSUHIM), has been subjected to extensive validation using published cadaveric test data including the intracranial and ventricular pressure data reported by Nahum et al. [97] and Trosseille et al. [140], the relative displacement data between the brain and the skull by King et al. [67] and Hardy et al. [46], and the facial impact data by Nyquist et al. [102] and Allsop et al. [4].

Although it is known that human brain tissue consists of a network of neurons, axons, arterioles, capillaries, and venules interspersed within a matrix of supporting cells; none of the aforementioned models had sufficient mesh resolution to replicate this complex architecture. In order to consider the effect of tethering due to the blood vessels and other structures, material properties of the brain used in head models have typically assumed a higher value than those reported from direct measurements of in vitro specimens dissected from cadaveric or animal subjects. However, to include all of the major vasculature in a 3D brain model is a significant modeling challenge. Zhang et al. [159] developed a 2D FE model of the human head, consisting of the skull, dura matter, CSF, tentorium, brain tissue, and the parasagittal bridging veins, and a second 2D FE model which also included major branches of the cerebral arteries. The authors found that the maximum principal strain/stress in the brain was lower in the model that included simulated blood vessels. The inclusion of the cerebral vessels added regional strength to the brain substance, and thereby contributed to the load bearing capacity of this composite brain model during head impact, analogous to reinforcing bars in a reinforced concrete structure. Unfortunately, incorporation of blood vessels in a 3D FE head model is not practical at this stage due to the lack of computing power.

Up to this point, data generated by all head models described above had never been correlated with injuries seen in living humans. Because the testing of volunteers cannot be taken to an injurious level, contact sports and real world car crash events present a unique opportunity to overcome this shortcoming. Through collaboration with the US National Football League (NFL), 24 head-to-head field collisions were simulated using the WSUHIM. Several injury predictors and injury levels were analyzed by correlating brain tissue responses with the site and occurrence of mild traumatic brain injury (concussion) seen in the field. Results indicated that the shear stress around the brainstem region could be an injury predictor for concussion. Viano et al. [144] further analyzed strain responses occurring at specific time points during and after impact and compared with the signs and symptoms of concussion seen in these players. They found that locations with the largest strains significantly correlated with the removal from play, cognitive and memory problems, and loss of consciousness observed in injured players. Additionally, concussive injuries occur during the rapid displacement and

rotation of the cranium, after peak head acceleration and momentum transfer in helmeted impacts.

In another study, Franklyn et al. [35] recreated four real-world full-vehicle automotive side impact cases at a proving ground. The cases were selected from an Australian crash sampling database. Head kinematics (three translational and three angular velocities) measured during the crashes were used as inputs to both the WSUHIM and the National Highway Traffic Safety Administration (NHTSA) Simulated Injury Monitor (SIMon)—detailed in the next section—to determine model-predicted injury outcomes, which were then compared with known location of severity of brain injuries received by the real-world occupants. The results demonstrated that both models were capable of predicting varying injury severities (i.e., varying AIS injury levels) in the real-world cases. The WSUHIM predicted a slightly higher injury threshold than the SIMon, probably due to the finer mesh and different software used for the simulations. Additionally, the WSUHIM could be used to determine regions of the brain which had been injured, although the computer resources needed to run this model were much more than those required by the SIMon model.

Furthermore, the WSUHIM was also used to improve automotive hood design. In order to reduce the risk of brain injury during head-to-car-hood impact in pedestrian crash, a collaborative study between WSU and Autoliv was conducted to investigate the influence of impact speed on head and brain injury risk (Fredriksson et al. [37]). Head kinematics generated from headform-hood contact was used as input to the WSUHIM. Results of this study showed that: (1) a lower head injury criterion (HIC) value did not always reduce the risk for brain injury and (2) a under-hood clearances of 60 mm in 20 km/h and 80 mm in 30 km/h impacts reduced the risk of skull fracture and brain injury significantly.

5 National Highway Traffic Safety Administration

Brain models are also being considered by NHTSA for potential rule making in the US. To upgrade the HIC-based head injury standard, NHTSA worked on a brain model which could calculate brain strain based on head kinematics measured from crash test dummies, thereby giving a more complex picture of brain injuries from non-accelerative mechanisms. A simple model “SIMon I” with a non-deformable skull was developed to minimize run time so that it can be used by original equipment manufacturers who routinely conduct a large number of crash tests. The NHTSA model was originally developed by DiMasi et al. [27] and later modified by Bandak and Eppinger [30] and DiMasi et al. [28]. This model contained only the cerebrum and had a very thick falx (average 7 mm) to avoid poor quality meshes typically associated with a low aspect ratio. A slip interface with a low coefficient of friction was introduced between the interior dura and external surface of the cortex to facilitate brain motion. The authors further hypothesized that the risk of sustaining a diffuse axonal injury was

proportional to the fraction of the brain volume which exceeded a preset injury threshold. Simulation results indicated that HIC was sensitive to translational kinematics only, whereas cumulated strain damage measure (CSDM) responded to rotation or combined translational and rotational conditions. Bandak [7] and Bandak et al. [8] further developed techniques to allow users to develop FE head models from biomedical images with ease. Their model also emphasized the simulation of skull fracture.

To improve the mesh quality of this model, Takhounts et al. [134] extended and rounded the lower part of the cerebrum of the previous SIMon model to avoid stress concentrations. The authors tested several nonlinear material models, including the Ogden rubber and Mooney–Rivlin rubber, and concluded that the linear viscoelastic material law was the best available approximation at the time. Based on a logistic regression of the model-predicted responses and animal injury outcomes, the authors derived three injury measures to estimate the risk associated with three different injury types: (a) a cumulative strain damage measure (CSDM) exceeding 55% of the brain volume represented serious risk of sustaining diffuse axonal injury (DAI), (b) a dilatation damage measure (DDM) of lower than -100 kPa (tension) represented an occurrence of brain contusion and focal lesions, and (c) a relative motion damage measure (RMDM) of one corresponded to the occurrence of an acute subdural hematoma (ASDH). The authors also found that side impact was potentially more injurious than frontal impact due to the more severe rotational kinematics.

A new geometrically detailed FE head model comprised of the cerebrum, cerebellum, falx, tentorium, pia-arachnoid complex with CSF, ventricles, brain-stem, and parasagittal blood vessels was developed based on the SIMon concept [135]. The new model represented the brain of a 50th percentile male and can be used to simulate combined translational and rotational accelerations of up to $400g$ and $24,000$ rad/s². The model was used to simulate mild TBI cases in American football players at the collegiate level to derive injury thresholds before it was used to investigate brain injury potential in NHTSA conducted side impact tests.

6 Université Louis Pasteur of Strasbourg

In France, Trosseille et al. [140] conducted five cadaveric head impact tests to provide much needed cadaveric data that can be used for model validation. They also used a 2D sagittal plane model developed by Lighthall et al. [83] to determine the effect of material properties on model-predicted responses. Other French human head models came mostly from Université Louis Pasteur of Strasbourg (ULP) where the initial emphasis was on finding the natural frequencies of the head in order to design protective devices that can prevent the head from being exposed to these resonant frequencies [149, 150]. Constant energy shocks of varying duration were used as input to the model and the

resulting compressive, tensile, and shear stresses, along with the relative brain–skull displacement and skull deformation were evaluated. Turquier et al. [142] used the head model developed by Willinger et al. [151] based on MRI scans to simulate the experiments conducted by Trosseille et al. [140]. The model-predicted responses (in terms of three intracranial accelerations measured at the lenticular nucleus as well as frontal and occipital lobes, three epidural pressures measured at the frontal, occipital, and temporal regions, and two intracranial pressures measured at the third and lateral ventricles) matched experimental results in terms of trend but showed significant oscillations. After introducing damping into the model, numerical oscillations were only slightly reduced. The authors called for more investigation into the assumptions used to model the subarachnoid space.

A short time later, Kang et al. [61] reported another model, which corrected the simplified geometry used in modeling the temporal lobe developed previously by Willinger et al. [149], and validated it against the intracranial pressure data reported by Nahum et al. [97]. A helmeted Hybrid II headform was used in a series of drop tests to reconstruct a real-world head impact of a motorcyclist into a Range Rover. The motorcyclist suffered a severe contusion to the right temporal lobe, tentorial contusion and subarachnoid hematoma over the occipital lobe, and laceration of the brainstem. Kinematics from the best correlated test—defined as the best match of the impact location and helmet damage—were used as input to the model to predict intracranial responses. The authors reported that shear stress correlated the best with the reported right temporal contusion observed in autopsy. Willinger et al. [152] further used the model to simulate cadaver test results. Although the model-predicted responses matched well against data from the short duration test, they did not match those obtained from a long duration impact. The authors emphasized the need to validate the FE head models against a variety of impact conditions to minimize errors.

Raul et al. [110] extended the application of the ULP head model from simulating automotive-induced head injuries to fall-induced head injuries of a 63-year-old male who fell backward to a wooden floor after being pushed by another person and then fell again from an emergency cart during lifting of the victim to the fire truck. The estimated impact velocity was 6 and 1.5 m/s for the first and second fall, respectively. The authors believed that the model-predicted responses could be used to exclude those injury mechanisms that were not likely in causing the injury seen in this case. Raul et al. [111] further suggested that FE human head models should be used routinely in forensic medicine. Marjoux et al. [89] reconstructed 61 real-world head injury cases experimentally and numerically to compare the predictive performance of using HIC, head impact power (HIP) proposed by Newman et al. [101], the CSDM, DDM, RMDM computed by the SIMon model [134], and intracranial responses predicted by the ULP model [61] as the injury mechanism. The authors concluded that moderate and severe brain injuries can only be distinguished with numerical model-based criteria and not with external (global) head acceleration.

7 Royal Institute of Technology (KTH) of Sweden

The geometries of most FE head models are taken from an idealized or a representative single subject's anatomy. Kleiven and von Holst [68] developed a parameterized human head and a simplified neck model to allow rapid changes in the model geometry. The model was validated against intracranial pressure data measured by Nahum et al. [97]. Six models of different sizes, representing a small female, a 5th percentile female, a 50th percentile female, a 50th percentile male, a 95th percentile male, and a large male were created to study the effect of head size in terms of von Mises stresses and HIC for padded frontal impacts and inertial loading. The authors found more than a fourfold increase in the peak stress while the HIC decreased 43% when the head size was increased from the smallest to the largest. They suggested that the size dependency was not reflected by HIC and recommended that any new head injury criterion should include the variations in head size. Ruan and Prasad [123] in their comments on this KTH model indicated that the negative pressure was too low (nearly -280 kPa) which may invalidate the findings of this study.

Again considering global response parameters, Kleiven [70, 71] compared FE model predicted intracranial responses to HIC and HIP from nine different applied pure translational and rotational acceleration pulses. He found that HIC responded in accordance with the magnitude of translational acceleration, but was not influenced by pure rotational impulse, while HIP required individual scaling coefficients for the different terms to account for different loading directions. Additionally, the largest bridging vein motion occurred in the shortest bridging veins, specifically those that were oriented in the plane of the motion and were angled in the direction of motion during rotation of the head in the sagittal plane. Following this train of thought, bridging vein geometry would significantly affect the strain in the bridging veins and may present a substantial obstacle for researchers to create subject-specific model suitable for predicting bridging vein rupture and associated injuries.

A variation on these models, Kleiven and Hardy [69] presented a FE head model which appeared to resemble the model reported by Kleiven and von Holst [68], but was "substantially different" from it according to Kleiven and von Holst (2006). The model used a hyperelastic Mooney–Rivlin linear viscoelastic constitutive law to simulate the brain and a selective reduced integration (SRI) scheme instead of the commonly used reduced integration scheme. Their model predicted a smaller relative motion between the brain and skull due to a lateral impact as compared with frontal or occipital impacts, consistent with the experimental data obtained by Hardy et al. [47]. A tied interface definition to represent the CSF resulted in model predictions which best correlated with measured intracranial pressures. However, the combination of a SRI scheme, Mooney–Rivlin material model, and a tied interface was later challenged by Takhounts et al. [134]. These authors speculated that the SRI scheme was susceptible to shear locking and was less stable than the reduced integration methods. Additionally, the

Mooney–Rivlin model did not match material properties obtained experimentally. Perhaps these numerical procedures were model specific, thus making it more difficult for researchers to decide from the literature what to follow when attempting to develop a reliable brain injury model.

To investigate localized anatomical effects, Ho and Kleiven [48] developed a 3D head model in which major arteries and veins were represented by “beam” elements to study the effect of cerebral vasculature on brain response. Differences in maximum principal strain predicted by models with and without vasculature were no more than 4% of the peak maximum principal strain. The predicted peak differences in strain between the model with and without vasculature were lower than those reported by Zhang et al. [159] using their 2D model which included Explicit modeling of the cerebral arteries. Ho and Kleiven [48] believed that the difference was due to the high vessel-to-brain volume ratio used in Zhang’s model as well as the high vascular density in the para-sagittal plane selected by Zhang and the low vascular density in their 3D study. Nevertheless, the authors found that vessel-induced strain reduction in regions representing the thalamus and corpus callosum were higher than other regions, indicating that the effect of cerebral vasculature could be highly localized, rendering it more difficult to model brain vasculature accurately. Additionally, Ho and Kleiven [49] developed two highly detailed FE models, one with and one without sulci (a network of folds that cover the brain surface), with an average element size of about 1 mm³. The models were loaded in three configurations: translational acceleration in the sagittal plane, rotational acceleration in the coronal plane, and rotational acceleration in the sagittal plane. Except for the parietal lobe in sagittal and coronal rotation accelerations, the model with sulci predicted a lower peak maximum principal strain when compared to the model without. The authors suggested that future FE brain model should include the sulci because this anatomical feature could significantly alter the strain distribution pattern.

For comparison to real-world injury, Kleiven [72] simulated NFL collisions, in which 25 players had concussion and 23 without, and a motorcycle accident, in which the rider sustained severe hematomas. The model used to reconstruct these cases was the same as that published previously [69, 72]. A series of parametric studies was conducted to show the effect of different material properties selected to represent brain tissues. Aside from intracranial responses predicted by the model, global injury measures (e.g. peak angular and translational acceleration, angular velocity change, HIP, and HIC) were also calculated. He found that the maximal pressure in the gray matter correlated best with injury while the maximal principal strain could be used to identify the location of injury observed in the motorcyclist. After testing several combined injury measures, the author found that a linear combination of HIC and peak change in rotational velocity correlated best with model-predicted maximum principal strain.

8 Eindhoven University of Technology (TUE)

Claessens et al. [22] created a coarse mesh model with geometry based on the Visible Human Data available at the U.S. National Library of Medicine. Because the brain and skull were directly coupled, the model failed to predict the intracranial pressures reported by Nahum et al. [97]. Better correlation with experimental data was achieved after adding a layer of friction-free contact interface between the brain and the skull. A more detailed model was also developed to include the falx, tentorium, and brainstem in the same report. Although experimental data on relative motion between the brain and the skull were not available at that time, the authors concluded that the junction between the brain and skull was somewhere between the rigid coupling and the free interface they simulated. However, they suggested that the coupling would be closer to a free interface. Brands et al. [11] continued this modeling effort by transforming Claessens's model into a MADYMO (version 5.4.1) model which used a reduced integration scheme. Before using this nonlinear model, a physical gel model was tested and modeled. After the authors matched the gel experimental results against model predictions, nonlinear "strain softening" viscoelastic properties for the human brain were derived and incorporated into the model. The motion of brain tissue through the foramen magnum was suppressed. Still, the model predicted a maximum shear strain which was ten times that reported by Bandak and Eppinger [6] when the same loading condition was applied. The authors attributed this increase in strain to the low shear modulus and strain softening effect they assumed in their model simulations.

A 2D plane strain model was developed from MRI data by Kuijpers et al. [75] to study the influence of linear elastic or viscoelastic brain material properties, different contact conditions at the skull-brain interface, and incorporation of a neck constraint. They found that intracranial pressures were more sensitive to the type of skull-brain interface condition than to the presence or absence of a force-free foramen magnum. Additionally, constraints in the neck affected the deformation of the brain but different time-dependent deviatoric material parameters did not significantly change the response. Cloots et al. [23] speculated that the convolutions of the cerebral cortex could affect the cortical stresses and strains. Several highly detailed substructure 2D models containing gyri and sulci were developed and loaded by the boundary conditions generated from the model reported by Brands et al. [11]. Results indicated that inclusion of the gyri and sulci had no significant effect on the mean von Mises stress, but had a significant effect on the maximum value.

9 Other Institutions

Numerous institutions throughout the world also developed human head models for impact simulations. Idealized models and simplified physical surrogates with accompanying models have also been reported. At the Medical College of

Wisconsin (MCW), Pintar et al. [104] developed a simplified spherical FE model to represent the human skull and brain and then used it to simulate penetrating head injuries by two different types of projectiles. Five years later, Zhang et al. [157] applied head kinematics measured from Hybrid III and EuroSID-2 dummies to the NHTSA SIMon model to estimate the risk of brain injuries. A total of 13 frontal and 20 side impacts without head contact and with low HIC (less than 1,000) were simulated. The authors concluded that more than 80% of the brain strains were contributed by rotational acceleration and recommended that rotational accelerations should be quantified in future crash tests to improve occupant safety. Additional research was performed by Yoganandan et al. [156], who used the same simplified 2D human brain model reported by Li et al. [82] and mentioned previously to subject the brain to four different angular acceleration pulses. The brain was subdivided into 17 regions and the average model-predicted maximum principal strains for each region was presented. The highest strains were found in corpus callosum while the lowest strains were found in the lower parietal lobes and the shape of acceleration pulses had a profound effect on the regional intracranial strain.

In Taiwan, Chu et al. [21] reported a 2D plane-strain model and validated it against pressure data by Nahum et al. [97] and resonant frequencies reported in the literature. The authors identified that shear strain better predicted cerebral contusion than intracranial pressure. Kurosawa et al. [77] in Japan reported a simple cylindrical model consisting of an acrylic container (skull), water (CSF), and agar (brain). However, the pressure they predicted was too high. Johnson and Young [60] in UK segmented the skull from high-resolution MR images of a volunteer and then used the data to rapidly prototype a plastic skull. A pendulum was used to impact the plastic skull filled with water to represent the brain. A FE model representing the same skull was also created and simulation results matched well with those obtained experimentally. Although their study proved that a FE model could indeed duplicate experimental results, the plastic-skull and water-brain was far too simple to represent a human head. Sarron et al. [126] in France tested 30 human skulls filled with silicone gel to study the “rear effects” head injury, which is defined as injury induced by non-penetrating indentation of the military helmet during ballistic impact. A 3D FE model was used to conduct a parametric study, in which results showed that the diploë layer played a role in protecting the skull from fracture. In India, Kumaresan and Radhakrishnan [76] reported a 3D head model and calculated the first five modal frequencies and the maximum shear stress due to an occipital impact. Xu and Yang [155] in Changsha, China also reported a FE human head model in an article written in Chinese. This model also used experimental data reported by Nahum to validate the model.

Some 3D models have considered the role of the neck in brain kinematics. Zong et al. [166] in Dalian, China developed a simplified 3D head-and-neck model and validated it against intracranial pressure data obtained by Nahum et al. [97] and Trosseille et al. [140]. The model geometry appeared to have been adapted from Shugar [130] but the authors did not provide a clear indication regarding how the model geometry was obtained. A “structural intensity” method was used to indicate the power flow within the loaded structure. Although the title of this study

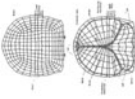
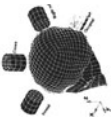



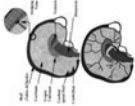
was related to head impact, the authors concluded that the spinal cord was vulnerable during the three impact scenarios simulated. Huang et al. [56] in Taiwan developed a 3D head model to simulate indirect impact due to flexion and extension about the upper cervical spine and found that intracranial pressures were lower in indirect impact compared to direct impact. They assumed that brain injuries also occurred in indirect impact (even though researchers have never produced any direct evidence of brain injury in real world cases), the authors concluded that shear strain is a better injury predictor compared to pressure. In Japan, Kimpara et al. [65] developed a 3D head–neck model consisting of major components of the head and cervical spine to investigate the biomechanical responses of the brain–spinal cord complex. The head–neck model was validated against three sets of brain test data obtained by Nahum et al. [97], Trosseille et al. [140], and Hardy et al. [46] and two sets of neck test data obtained from Thunnissen et al. [141] and Pintar et al. [104]. A series of parametric studies was conducted and results showed that a soft head contact or no head contact could reduce the CSDM predicted diffused axonal injury. The authors used the ultimate strains of the spinal cord and pia mater to estimate the risk of neck injury.

Automotive impacts have also been investigated in models not yet described. Horgan and Gilchrist [52] in Ireland developed a 3D head model for simulating pedestrian accidents. The intracranial pressure was validated against Nahum et al.'s experiment [97]. Parametric studies regarding the effect of different mesh densities and influence of material properties were performed. The authors found that the short-term shear modulus of the brain tissue had the biggest effect on intracranial frontal pressure, and on the Von-Mises response. The bulk modulus of the CSF had a significant effect on the contre-coup pressure when the CSF was modeled. The coarse mesh model was fine for pressure prediction compared to a finer mesh. The authors also concluded that careful modeling of the CSF and skull thickness is necessary for correctly predicting intracranial pressure. Also, the FE head model is better to be scaled to the particular head being simulated for accurate prediction. A version of this model was also used by Rousseau et al. [116] to investigate how changes in neck kinematics affect brain tissue strain. It was found that increased neckform compliance increased maximal principal strains in the cerebellum, but no effect was seen in other brain regions when increasing or decreasing compliance. The authors stated difficulties in applying their findings to brain injury due to a lack of established threshold. Krabbel and Appel [74] in Germany developed a 3D human cranium model from CT scans. Kinematics of a Hybrid III head due to frontal impact and a EuroSID I due to lateral impact were calculated from MAD-YMO and used as input to the skull model. No injury assessment was reported.

10 Summary of Blunt Impact Brain Models



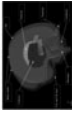



Based on the literature review discussed above, a summary of key FE adult human head/brain models developed for blunt impact simulations is presented in Table 1.

Table 1 Summary of FE adult human head/brain models

First author, year	Ruan et al. [117]	Ruan et al. [118, 119]	Zhou et al. [163]	Al-Bsharat et al. [2]	Zhang et al. [159]	Zhang et al. [160, 161]
Institute	WSU					
Mesh						
Part	Head	Head	Head	Head	Head	Head
Solving software	MARC, ANSYS	PAM-CRASH	PAM-CRASH	PAM-CRASH	PAM-CRASH	PAM-CRASH
2D/3D	2D	3D	3D	3D	3D	2D
Geometry	50th percentile human head geometry	Average adult male head geometry	50th percentile adult male head geometry	50th percentile adult male head geometry	50th percentile male head, anatomical drawings	Anatomical drawings
Elements	Shell	Hexahedral elements: brain 1,760, skull 2,800, CSF 896	22,995 elements. Total mass 4.37 kg with brain being 1.41 kg	41,354 elements. Total mass of 4.3 kg.	314,500 elements with a mass of 4.5 kg	Model I and II, 4,501 elements with a mass of 41.07 g
		Shell elements: scalp 864, dura 896, falx 135.				

(continued)

Table 1 (continued)

First author, year	Ruan et al. [118, 119] [117]	Zhou et al. [163]	Al-Bsharat et al. [2] [160, 161]	Zhang et al. [159]		
Material law	Elastic material for brain and skull Linear viscoelastic material for brain, Elastic-plastic material for bone, elastic material for the remaining	Similar to Ruan [119]	Similar to Zhou [163]	Linear viscoelastic material for brain, linear elastic elements for vessels Linear viscoelastic material for brain, elastic-plastic material for bones, elastic material for membrane, skin, cartilage		
Validation	No	Intracranial pressure	Intracranial pressure, Perform comparison of skull-brain relative displacements from FE model and experiment	Intracranial pressure, Intracranial pressure, brain/skull relative motion		
First author, year	Ward [148, 147, 145]	Dimasi et al. [27] Bandaq et al. [6] Dimasi et al. [28]	Takhoumts et al. [135]	Willinger et al. [149] Kang et al. [61]	Classens et al. [22]	
Institute	Biodynamics/Engineering Inc.	NHTSA		ULP	TUE	
Mesh						
Part	Head	Head	Head	Head	Head	

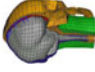

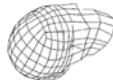


(continued)

Table 1 (continued)

First author, year	Ward [148, 147, 145]	Dimasi et al. [27]	Takhounts et al. [135]	Willinger et al. [149]	Kang et al. [61]	Claessens et al. [22]
Solving software	SAPIV, SAPV	LS-DYNA	LS-DYNA	NA	NA	MARC
2D/3D	3D	3D	3D	2D	3D	3D
Geometry	Atlas	Anatomical slice data	CT scan of 50th percentile male	NA	Lab obtained skull geometry and atlas	CT and MRI
Elements	Coarse hexahedral elements	Approximately 5,900 elements	5153 shell, 40,708 hexahedral elements, 14 bean elements	573 plane strain elements	10,395 hexahedral elements, 2,813 shells, with total mass of 4.7 kg	1,756 hexahedral elements, with total mass 3.1 kg
Material law	Elastic material	Linear viscoelastic material for brain, elastic material for membrane, rigid skull	Linear viscoelastic material for brain and PAC-CSF, elastic fluid for ventricle, elastic material for membrane, cable discrete beam for vessels, rigid skull	Elastic material for brain, bone. Membrane neglected	Linear viscoelastic material for brain, elastic material for CSF, scalp, membrane, and facial bone, elastic brittle property for composite skull	Linear elastic material for brain and skull
Validation	Intracranial pressure	Intracranial pressure	Intracranial pressure, No Brain/skull relative motion	No	Intracranial pressure	Intracranial pressure


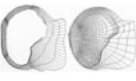




(continued)

Table 1 (continued)

First author, Year	Ho et al. [49]	Chu et al. [21]	Huang et al. [56]	Kimpara et al. [65]	Horgan et al. [52]
Institute	KTH	National Yang-Ming Medical College, Taiwan	Taipei Medical College, Taiwan	Toyota Central R&D Labs., Inc	University College Dublin, Ireland
Mesh					
Part	Head	Head	Head	Head	Head
Solving software	LS-DYNA	ANSYS	ANSYS	LS-DYNA	ABAQUS
2D/3D	3D	2D	3D	3D	3D
Geometry	NA	Atlas	Modified from Shugar's model	THUMS-AM50	CT
Elements	11,454 hexahedral elements, 6,940 four-node elements, 22 two-node truss elements	Average element size 1 mm ³ , with brain mass around 1.2 kg	1,328 solid elements (including 60 four-node pyramids and 24 five-node tetrahedral elements), with brain mass 1.307 kg and total mass 2.932 kg	49,579 solid elements, 25,119 shell, and 364 seatbelt element, with a total mass as 4.39 kg	Element densities varying from 9,000 elements to 50,000 elements

(continued)

Table 1 (continued)

First author, Year	Kleiven [68]	Ho et al. [49]	Chu et al. [21]	Huang et al. [56]	Kimpara et al. [65]	Horgan et al. [52]
Material law	Hyperelastic and viscoelastic material for brain tissue, linear elastic for bone, scalp, and membrane	Ogden hyperelastic material for brain, elastic fluid for CSF, quasilinear viscoelastic shell for pia, simplified rubber/foam material for falx and tentorium, rigid skull, Brain/skull relative motion	Linear elastic material for brain and skull	Linear elastic material for brain and skull	Elastic-plastic material for bone, linear viscoelastic material for brain, elastic material for membrane	Linear viscoelastic for brain tissue, hybrid elements for CSF, elastic material for bone and scalp
Validation	Intracranial pressure, Brain/skull relative motion	Brain/skull relative motion	Intracranial pressure	Intracranial pressure	Intracranial pressure, Brain/skull relative motion	Intracranial pressure
First author, year	Zong et al. [166]	Bandak [7]	Johnson et al. [60]	Krabbel et al. [74]	Cloots et al. [23]	Li et al. [82]
Institute	Dalian University of Technology, China	NHTSA	University of Exeter, UK	Technical University Berlin, Germany	TUE	MCW
Mesh						
Part	Head	Head bone	Head bone	Head bone	Cortex slice	Simple physical model

(continued)

Table 1 (continued)

First author, year	Zong et al. [166]	Bandak [7]	Johnson et al. [60]	Krabbel et al. [74]	Cloots et al. [23]	Li et al. [82]
Solving software	MSC/DYTRAN	LS-DYNA	LS-DYNA	PAM-CRASH	ABAQUS	ABAQUS
2D/3D	3D	3D	3D	3D	2D	2D
Geometry	NA	CT	MRI	CT	Topological study	Sphere
Elements	Minimum side length of the solid elements is 0.64 mm. Average side length is about several centimeters	Projection method used to generate high resolution and medium resolution models	Slightly over 200,000 heahedral and tetrahedral elements (head bone)	1,342 solid elements (head bone)	4,243–4,533 elements for heterogeneous models, 3,072 elements for homogeneous model	4,650 elements
Material law	All materials assumed as linear elastic	Lineat elastic material for bone, brain, scalp	NA	Elastic–plastic material for bone	Non-linear viscoelastic material for brain, low shear modulus elastic solid for CSF	Linear elastic for skull and falx, hydrodynamic material model for CSF, linear viscoelastic material for gel
Validation	Intracranial pressure	No	No	No	No	Motion and strain

WSU Wayne State University, *NHTSA* National Highway Traffic Safety Administration, *ULP* Université Louis Pasteur of Strasbourg, *KTH* Royal Institute of Technology of Sweden (Swedish: Kungliga Tekniska högskolan), *MCW* Medical College of Wisconsin, *TUE* Eindhoven University of Technology

The table lists the first author of the model developers and the year when the model reported. It also compares mesh, software, element type, and material laws used, model geometry and what data were used for model validation. Several key conclusions from this review are:

First, the complexity of human head models has been augmented significantly over the past two decades and each new version of the model was able to address additional clinical phenomena or to make site-specific correlation between the model results and real world injury. Even though all available data have been used for validation of the latest models, they can only be considered partially validated because the quantity and quality of these experimental data are still relatively low. Additionally, the shortage of quantitative material property data continues to prevent total validation. Nevertheless, useful information has been derived from model predictions. Two common conclusions can be drawn from these FE modeling studies: shear strain is mainly due to rotational impact, while intracranial pressures are affected mostly by translational acceleration and stiffness of the skull.

However, there are many unanswered issues which may hinder continued development of the human head model. For example, modeling of the pia-arachnoid complex, within which the CSF flows, continues to be an unresolved issue for many researchers. Among the techniques used to model this interface are a direct connection with no slip, direct coupling at the junction, sliding interface with different coefficients of friction, or tie-break with a preset threshold. Unfortunately, the method that best represents the real-world situation cannot be determined with confidence until the relative motion at this junction is actually measured. Nevertheless, most researchers reported that representing the CSF layer by a gap cannot be used to generate tension in the contre-coup site, thus making it unsuitable to model the contre-coup phenomenon reported by clinicians. Experimental data reported by Jin et al. [57–59] on bovine pia-arachnoid complex showed that the trabeculae in the CSF layer offers finite in-plane, traction, and shear resistance, thus it would be a mistake to model this layer as an incompressible fluid.

Second, variations in skull thickness are generally neglected in the simulation of closed head injuries. However, skull thickness is an important issue for direct impacts to the head because one cannot simply input head kinematics to the center of gravity of the head and expect to model skull fracture. Both its thickness and material properties have an effect on how or where a fracture would initiate. According to Ruan and Prasad [122], human skull thickness varied from 4 to 9 mm in five published studies, but all models so far have assumed a uniform thickness. Such information should be incorporated into the model for direct-impact simulations to reflect how local bone thickness affects bone fracture and transfer of energy to the brain. Also, it is necessary to include the scalp in direct-impact simulations because the scalp dampens an impact by increasing the duration and contact area over the skull.

Third, tissue level injury thresholds are unknown. It is a common trend to use the computed maximum principal strain or stress and pressure as an estimate for

the risk of head injury. Ruan and Prasad [120] suggested the use of a computed stress threshold (pressure or shear) to derive the head acceleration and impact duration for risk estimation. A maximum von Mises stress of 100 MPa in the skull was suggested as the threshold for skull fracture while a maximum shear stress of 22 kPa was the proposed threshold of a reversible concussion. With this method, the automotive designers can use measured dummy head kinematics to predict the risk of brain injury. However, it should be mentioned parenthetically that the use of von Mises stresses is a convenience but not necessarily a biomechanically valid parameter for predicting injury. Additionally, the CSDM, DDM, and RMDM proposed by NHTSA make physical sense because occurrence of high stress in a single element may not be a meaningful measure of injury to the brain due to numerical issues as well as physiological reasons. However, more research is needed to establish different injury thresholds for different brain tissues. For example, a 15% strain may be injurious to the brainstem, but not to the gray matter.

Fourth, high strain rate material properties of the brain remained the largest road block en route to accurate modeling of brain response. Selection of constitutive laws and their associated material constants varies greatly among different research groups. Until a set of realistic and commonly accepted properties becomes available, readers should be aware that a combination of incorrect input data can still yield a “correct” model prediction. This quest for proper material properties was identified by Goldsmith [41] more than 40 years ago and was reflected in the simplified FE model of skull and brain by Chan [16] that remotely resembled a human head. This issue has not been resolved as of today. For example, shear properties of the brain reported by Galford and McElhaney [38] and Prange et al. [108] differed by more than two orders of magnitude. Additionally, several researchers have reported a “strain softening” effect of the brain (i.e., shear stiffness decreases as the strain increases). This matter has been discussed by Brands et al. [10], Prange et al. [108] and Bilston et al. [9]. This phenomenon probably bears further study because the concept is counterintuitive and the phenomenon is not seen in other biological tissues. Nevertheless, the trend predicted by all models seems to be similar. In particular, intracranial pressure appears to be the easiest parameter to match by all groups, even though only a limited number of experimental datasets are available.

Finally, the predominant deficiency is the lack of experimental data to properly validate the model-predicted results against the impact responses of the head and brain. In terms of intracranial pressure, only a total of three datasets—two reported by Trosseille et al. [140] and one from the often-cited Test 37 reported by Nahum et al. [97]—are available to validate forehead impact. Similarly, only a few tests reported by Hardy et al. [46, 47] are available for the validation of the motion of the brain relative to the skull. Additionally, for a comparison of model response to human injury, there are some 30 cases of mTBI reconstructed from NFL games [144] and four sets of graded AIS scale head injury derived from real world crashes reported by Franklyn et al. [35]. Other real world situations are not well-documented enough for this purpose. New and higher quality experimental or real

world data are needed for the continued improvement of simulation models to enhance their capability in accurately predicting the risk of brain injury under a given blunt impact condition.

10.1 Blast-Induced Brain Injury Models

Blast neurotrauma has become the “signature wound” of the current Mideast conflict due to exposure to improvised explosive devices [42, 103, 167]. Victims of blast-related TBI suffer from complex neuropsychiatric symptoms such as dyspraxia, dysphasia, executive dysfunctions, paralysis, deficits, and dysfunctions of special senses, and mood disorders [32, 84]. This type of blast-related brain injury is categorized as primary because it is related directly to the shock wave itself, as opposed to subsequent insults. Brain injuries resulting from fragments caused by blast are classified as secondary, and those caused by impacts with objects when the individual is propelled through space are termed tertiary [32, 84]. Secondary and tertiary TBI are the result of blunt trauma routinely seen in falls, vehicle crashes or contact sports, and have been studied with some degree of success over the past seven decades, and related computational brain models are summarized in the Blunt Impact section. In this section, the focus is on primary blast injury, as its mechanism is poorly understood, and the injury threshold remains unknown. In recent years, efforts have been made to study the effects of primary blast brain injury using FE models.

Compared with blunt head impacts, blast loading has a very short duration and very rapid pressure change. Because the magnitude of strains generated by these extremely short duration impacts is minuscule, many researchers hypothesize that pressure or pressure gradient is the mechanism of primary blast-induced brain injury. Currently, there exist several unvalidated blast related brain injury models, and the current status of their development is briefly presented below. Because this is a current above-the-horizon topic, this review also includes reports published in conference proceedings that may not have been rigorously peer-reviewed.

Unlike other hallmark blast injuries (such as blast lung), primary brain injury mechanism and tolerance have not been clearly established in terms of exposure. To investigate blast-induced brain injury mechanisms, Chafi et al. [12] developed a LS-DYNA head model consisting of all essential anatomical features (i.e. brain, falx and tentorium, CSF, dura matter, pia mater and skull) and used it to simulate primary blast brain injury. Material properties were taken from the published literature and the input was a blast created by 13 kg of C4 explosive at a distance of 3 m. High compressive stresses were observed in the frontal and parietal regions, while tensile stresses were large in the posterior fossa and occipital regions. They hypothesized that the pressure gradient might be responsible for brain damage. The same authors [13] also investigated the effect of shear stress using the same head model which was exposed to smaller charges (0.5 and 1.0 lb TNT). They compared the predicted stress level with published impact injury

thresholds and concluded that the deviatoric or shearing stresses developed at localized regions in the brain surrounding the ventricles might be the injury mechanism. The same authors [14] also reported the intracranial pressure gradient, shear stress, and principal strain when the model was exposed to overpressures in the range of 2.4 to 8.7 atmospheres. They suggested that it would be more appropriate to use an overall evaluation for injury prediction using various measurements instead of one single injury criterion. Additionally, they reported that dynamic responses of the brain were better injury predictors than head input accelerations.

Several other research groups have explored multiple mechanisms to determine which criteria may be most appropriate to establish blast loading tolerance. For example, Moss et al. [95] hypothesized that blast-induced head injury might be caused by secondary factors, such as forced relative motions between the skull and brain. An in-house software package was used to calculate the interaction between the shock wave and head, which was represented by a simplified elliptical solid with description of the skull, CSF, brain, and face. The model was exposed to a blast created by 2.3 kg of C4 at a distance of 4.6 m. They concluded that the likely cause of blast induced injuries was localized skull flexure with displacements in the order of 50 μm which generated a large pressure gradient in the underlying brain. Another model was developed by Zhang et al. [158] to study biomechanical responses, such as strain and displacement, within the brain. This idealized FE head model was exposed to a blast created by 10 kg of TNT at a distance of 1 m. Brain strains predicted in the coup and contre-coup regions were 4 to 7 times higher than that in the central region. Additionally, high brain strain (15%) and large deformations (4 mm) occurred in the brainstem region. From these results, the authors stated that there may be a higher probability of injury in the peripheral brain and brainstem regions due to blast overpressure loading. No consensus has been reached on the role of skull and brain displacement in blast-induced brain injury at this time.

Moore et al. [96] used an in-house fluid/solid coupling tool to simulate the detonation of 0.0648 and 0.324 kg TNT. A head model consisting of only the upper part of the head was used to calculate intracranial responses. The behavior of the brain tissue was described by a neo-Hookean elastic model with the Tait and Mie-Gruneisen equation of state Meyer et al. [92]. Results indicated that intracranial responses of an unprotected head with an intensity of 50% lethal dose blast lung injury were comparable to impact-induced mild TBI.

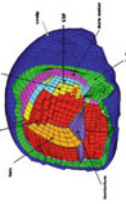
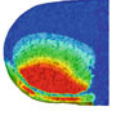
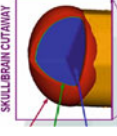

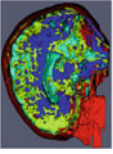
Other researchers have taken different approaches to simulate the blast event. Instead of using explosive simulations to produce shock waves, Taylor and Ford [137] applied an energized air flow with a peak pressure of 1.3 MPa as input to a head model developed from the Visible Human Female data set using a self-developed FE solver. Simulation results revealed that the blast-induced high pressure, shear stress and volumetric tension occurred within the first 2 ms of the blast exposure and was much too soon for any significant global motion of the head to take place. Consequently, the authors concluded that injury criteria based on linear and rotational accelerations were not suitable for evaluating

blast-induced TBI, indicating that this conclusion holds true whether the blast is simulated by explosives or by air flow alone.

Considering that there is currently no blast-related intracranial pressure data obtained from human cadavers for model validation, an FE model of the rat head subjected to air shock loading was developed and validated against the experimental data [165]. The rat head model was taken from a previously developed rat brain model for simulating blunt controlled cortical impacts [85] and described in more detail in the Animal Brain Model section. An FE model representing gas flow in a 0.305-m diameter shock tube was formulated using an Eulerian approach to provide input (incident) blast overpressures to the rat model. An arbitrary Lagrangian–Eulerian (ALE) fluid–structure coupling algorithm was then utilized to simulate the interaction between the shock wave and the rat head. The model-predicted pressure–time histories at the cortex and in the lateral ventricle of the rat were in reasonable agreement with those obtained experimentally. Further examination of the FE model predictions revealed that pressure amplification, caused by shock wave reflection at the interface of the materials with distinct wave impedances, was found in the skull. The overpressures in the anterior and posterior regions were 50% higher than those at the vertex and central regions, indicating a higher possibility of injuries in the coup and contre-coup sites. At an incident pressure of 85 kPa, the shear stresses and principal strains in the brain were at low levels, implying that they are not the main mechanism of injury in this particular scenario.

Table 2 briefly summarizes blast-related brain models developed and published to date. The table compares the mesh and geometry of the models, loading conditions applied, solvers, and parameters assessed. There are several key techniques involved include the mathematical description of the shock wave, fluid/solid coupling, and very high strain rate constitutive modeling, the details of which are beyond the scope of this chapter. Generally, it can be seen from Table 2 that at least three techniques were used in the simulation of fluid–structure interaction between the blast wave and the head, namely the multi-material ALE/Lagrangian coupling formulation, empirical pressure functions, and a pure Eulerian computational fluid dynamics algorithm. Shock wave/head coupling was implemented either by using commercially available software (i.e. LS-DYNA) or in-house computational tools. Intracranial pressure gradients, stress (compressive, tensile or shear), as well as shear strain were used to quantify the response of the head under shock loading. Despite the fact that these modeling efforts are aimed at providing relevant information in using computer models to study blast-induced primary brain injury, these reported models are far from perfect. All studies applied quasi-static material properties from the literature without consideration of the high strain rates involved in blast loading. Except the rat brain model reported by Zhu et al. [165], no other models were validated against experimental data pertaining to simulated blast loadings due to a paucity of such data. Based on aforementioned modeling results, several key parameters need to be measured during blast experiments in order to fully validate model predictions: (a) strain or deformation

Table 2 Brief summary of FE models developed to simulate blast-induced brain injuries

First author, year	Chafi et al. [12]	Chafi et al. [14]	Moore et al. [96]	Moss et al. [95]	Zhang et al. [158]	Taylor et al. [137]
Mesh						
Loading condition	13 kg C4 at 3 m 0.454 kg TNT at 0.8 m	0.038, 0.093 and 0.227 kg TNT at 0.8 m	0.0648 kg and 0.324 kg TNT at 0.6 m	2.3 kg C4 at 4.6 m	10 kg TNT at 1 m	Energized air flow with the peak pressure of 1.3 MPa
Loading modeling method	Multi-material ALE/Lagrangian coupling	Multi-material ALE/Lagrangian coupling	Multi-material ALE/Lagrangian coupling	Multi-material ALE/Lagrangian coupling	Empirical pressure equation (ConWep)	Pure Eulerian (CFD)
Geometry	Human head with detailed anatomy: Brain, falx and tentorium, CSF, dura mater, pia mater, skull bone, scalp	Human head with detailed anatomy (only upper part): Skull, ventricle, glia, white and gray matters, eyes, venous sinus, CSF, air sinus, muscle, skin/fat	Human head with detailed anatomy: Skull, CSF, brain and face	Simplified model: skull, CSF, brain and face	Simplified model: Skull, left and right lobes, and neck	Human head with detailed anatomy: Skull, white and gray matters, CSF
Solver	LS-DYNA	In-house software	In-house software	In-house software	LS-DYNA	In-house software
Parameters assessed	Compressive and tensile stresses	Shear stress	Intracranial pressure gradient, shear stress and shear strain	Pressure and maximum principal strain	Pressure and maximum principal strain	Volumetric tension, shear stress and pressure

of the skull and (b) pressures at multiple locations such as the coup, central, and contre-coup sites.

Additionally, there is no standard set of experimental data using a phantom (physical surrogate) to verify the biofidelity of software developed to calculate blast-induced intracranial response. While some researchers have commented the oversimplification and associated inaccuracies of certain commercially available software for blast simulations, none have provided a common dataset to check the accuracy of such software. Besides, there is a need to use a very fine mesh model to correctly simulate the thickness and density of the shock front and the solid–fluid coupling algorithms are very computationally expensive. Unfortunately, a model incorporated these features cannot be run with reasonable turnaround time at present. Improvements in modeling techniques, determinations of material properties at appropriate loading rates, accurate measurements of biomechanical responses in skull and brain, and faster computer are needed to comprehensively verify and validate FE models as a reliable tool in blast-induced brain injury research in future.

10.2 Pediatric Head and Brain Models

Although many lack the sophistication of adult FE head/brain models, several pediatric head and brain models have been developed to investigate biomechanical response with particular relevance to children. Major obstacles in this field are the lack of accurate material properties obtained from pediatric specimens and appropriate datasets for model validation. Each of these models was developed for distinctly different purposes, even though some age groups overlap, and as such, it is not relevant to directly compare predicted response values, especially in computational models which cannot be properly validated. Nevertheless, parametric studies using these models and comparative analyses of simulated results from these models can still provide useful information on pediatric head/brain injuries.

Some pediatric head models have been developed to study the effects of the more compliant infant skull on brain response. The first such model by Thibault et al. [138] utilized a simplified geometrical representation and different techniques for modeling the cranial sutures. They showed that, in a geometrically simple model meant to represent the infant brain as solid elements and the infant skull as shell elements, the maximum principal strain distributions of the intracranial contents were affected by the material properties of a thin, linearly elastic skull. A similar semi-ellipsoidal model by Kurtz et al. [78] used 1D springs to simulate sutures without fontanels (which may not be anatomically correct for the 3-month-old material property data used) and expanded the skull behavior to include plasticity. The linear springs allowed the sutures to support tension, but not bending, which seems to be biomechanically counterintuitive. This model was not validated, but posterior impacts were reported to cause the highest brain strains. Lateral impacts showed skull deformation remote to the impact area and instigated diffuse patterns of strain in the brain.

Another model with idealized geometry was published by Margulies and Thibault [88] in which the sutures were represented by elastic shell elements. As with the previously mentioned simplified models, no CSF layer was considered. Identical brain properties were assigned to both models but the skull and sutures were assumed to have either adult or 1-month-old infant material properties. An oblique impact load was applied to investigate the effect of different cranial bone properties on the intracranial tissue deformation pattern. Results indicated that increased skull deformation in the infant head might lead to changes in strain distribution within the brain. More specifically, a similar impact scenario could yield diffuse bilateral strain in the infant but focal unilateral strain in the adult. Again, no validation was performed in either model. The use of boundary conditions along the flat edge to prevent any global translation or rotation in simulations might have affected the conclusions reached by the authors.

Prange et al. [107] created an infant (2-week-old) and an adult FE skull–brain models from 2D MRI slices, each representing a 2 mm thick coronal section, to study brain injury induced by rotational loading applied at a fixed pivot point approximately at level of the mid-cervical spine (C4–C5). For the infant model, the brain was assigned either adult or infant material properties while only the adult properties were used in the adult model. Maximum principal strains at five anatomical regions were analyzed, and it was concluded that the brain size had a greater effect on response than material properties, though both played a role. No statistical significance tests were performed. It should be pointed out that projecting a 2D slice to create a uniformly thick 3D model can produce results of questionable validity as far as 3D response is concerned.

More advanced, anatomically accurate models have also been developed for various purposes. Desantis-Klinich et al. [26] reconstructed real-world automotive frontal impact cases, in which concomitant skull and brain injuries were attributed to deploying passenger-side airbags, using a child restraint air bag interaction (CRABI) dummy. The authors also developed an anatomically realistic 6-month-old infant head FE model from digitized skull CT contours for the purpose of predicting skull fractures through a stress-based criterion without consideration of intracranial response. When simulating the real-world scenario based on bilateral loading from the CRABI reconstruction, the highest stresses were observed at the point of impact, while real-world injuries suggested fractures tend to occur at locations remote from the impact site. This inconsistency was not resolved even though a von Mises stress-based fracture tolerance was presented. Although the model was sensitive to changes in modulus of the elastic skull, different moduli were not assigned to different bones. The brain was modeled as linearly visco-elastic with a CSF layer, and a parametric study found that decreasing the bulk modulus of the brain affected total skull responses, while increasing long-term shear modulus increased head acceleration. Based on comparative responses of a CRABI and the infant FE models, the authors proposed alternative values that were different from the accepted injury assessment reference values (IARV) for the CRABI dummy (scaled from adult data). However, given the lack of validation in the infant FE model, the applicability of the proposed values is questionable.

The predicted corridors for injury measures such as HIC and acceleration were wider for the infant FE model and higher than the CRABI values.

Another FE model, developed for the purpose of investigating skull fracture from drops and falls, was published by Coats et al. [24]. The geometry of the model was obtained from MRI and CT image sets of a 5-week-old infant. The interaction between the 8-noded skull shell elements and the tetrahedral solid brain elements was defined as a frictional interface with no CSF. The sutures were modeled as membrane elements. The parameters assigned for the brain were based on Ogden formulation, the sutures were linearly elastic, and different orthotropic parameters were given to the occipital and parietal bones based on bending data. Occipital loading was applied to simulate a short fall, and several brain and suture properties were parameterized and compared to responses from baseline. Brain stiffness (μ) was investigated due to the fact that Prange and Margulies [109] found infant porcine brain tissue to be twice as stiff as adult porcine tissue. Therefore, the baseline μ -value was defined as two times that of the human adult value (257 Pa) measured by this research group. It was observed that using 257 or 559 Pa did not significantly affect skull stresses, but increasing the stiffness to four times baseline (another adult value from the literature) increased peak principal stress, peak force, and contact area by greater than 15%. The authors showed that variations in material incompressibility also affected the skull response. However, no analysis was presented on how to choose appropriate values for the pediatric brain. Parametric studies of the suture indicated that decreasing suture thickness had little to no effect on the skull, but widening the suture to an unrealistic 10 mm affected peak stress and contact area. Removing the suture entirely did not change the predictions of this model, which may be a consequence of suture morphology simplification. Qualitative validation was performed based on using ultimate stress as an indicator of fracture, but the exact location and orientation of the fracture was not considered, nor were measurable quantitative values such as impact force.

The previously mentioned models incorporated a completely homogeneous brain mass, with or without CSF. However, a more detailed 6-month-old head model developed at ULP [113, 114] included several brain structures such as the falx and tentorium. As the geometry was derived from CT imaging, the anatomical accuracy of these structures is assumed to be estimated from an anatomical atlas. Nodal connectivity was employed to define interaction between skull, CSF, and brain. The brain was linearly viscoelastic, while all other parameters were linearly elastic. Several studies have been performed using versions of this head model, but no validation has been presented. The first publication [113] attempted to reconstruct the two phases of shaken baby syndrome (SBS) separately by the oscillatory shaking and the blunt occipital impact when the child was released. Model-predicted pressure and von Mises stresses were found to be much higher in the impact case, while strain predicted in the bridging veins through relative motion was similar for both loading conditions. The 2008 paper [114] illustrated the differences in biomechanical responses between the infant head model and a structurally scaled version of the adult ULP head model with similar material definitions. Results from the two models indicated visibly different predictions of

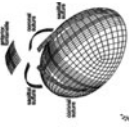
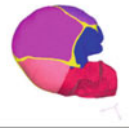
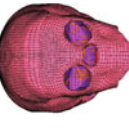


skull fracture location using a stress-based criterion for a single case history. However, due to rudimentary nature of this model, it does highlight the fact that children are not small adults, and that the biomechanical responses are both material and shape dependent.

The same researchers have also developed a 3-year-old head model using similar techniques to those of their 6-month-old model [115]. This 3-year-old head model was used to develop tolerance criteria for neurological lesions in real-world fall cases and two sets of brain material parameter values from the literature. In the absence of proper data for validation, 25 cases were used as a basis for statistical analysis of peak intracranial von Mises stress, peak internal pressure, peak angular and linear accelerations, and HIC using logistic regression risk curves. Based on an incomplete analysis in this study, HIC was shown to be the best predictor among different injury predictors. Variance in impact location was shown to affect the peak stress in the brain, as did a 30% error in fall height. However, it was concluded by the authors that the quantitative effect was within acceptable limits.

In addition to the study performed by Roth et al. [113], Couper and Albermani [25] also investigated SBS through FE modeling. In their study, a 2D model of a hemi-spherical brain MRI slice from a 3-month-old was developed, and more complex material properties compared to other published pediatric brain models were assigned. The constitutive model employed a nonlinear μ coefficient for the Odgen portion and various dissipation modes in the Maxwell element, with gray matter and three different myelinated white matters being assigned different properties. These values were estimated from published human and animal data for both adults and infants. Various subarachnoid space representations were also considered. The input to the model was an oscillatory acceleration, and the different simulation conditions were shown to have dissimilar biomechanical response. Simulated results from models without validation made it difficult for the authors to draw conclusions. Nevertheless, the authors postulated that using solid Lagrangian elements for the CSF layer is not appropriate for cyclic loading schemes based on phase differences. The volume of CSF is shown to have a large effect on brain response and is therefore an important factor in predicting brain injury. Although material properties are important, it was shown that the stress path may be more sensitive to the brain interface than to material stiffness based on this unvalidated model.

Table 3 lists a summary of the pediatric head and brain models discussed above, in terms of mesh, age, solving software, geometry, elements and material used, and validation status. Although the lack of proper validation in these models and the scarcity of appropriately documented injury criteria for children negates the possibility of drawing concise conclusions on injury risk, these models may point scientists and engineers in the direction of future pediatric brain injury research. It is interesting to note that brain material behavior often has been considered only secondary to the braincase itself, and that many of the FE model results show less effect from suture stiffness than might be expected. A recent review of directly measured pediatric material properties [36] indicates that such

Table 3 Summary of FE pediatric head/brain models

First author, year	(DeSantis) Margulies and Thibault [88]	Roth et al. [113, 114, 115]	Coats et al. [24]	Couper et al. [25]	Prange et al. [107]
Mesh					
Age	3 months	6 months	6 months and 3 years (2009)	1.5 months	3 months
Solving software	LS-DYNA3D	LS-DYNA	Radioss	ABAQUS/Explicit	PATRAN
2D/3D	3D	3D	3D	3D	Pseudo 3D
Geometry	Idealized	CT of 27 week subject; facial geometry from Zygote model	CT of 6 month and 3 year subjects	CT and MRI of 5 week old subject; suture geometry idealized	MRI of 3 month subject
Elements	25,279 solid elements, 5,514 shell elements, 137 springs	NA	6 MO: 69,324 solid elements, 9,187 shell elements 3 YO: 23,000 solid elements, 3,500 shell elements	11,066 tetrahedral solid elements, 624 hexagonal solid elements, 18,706 shell elements, 2,485 membrane elements	4,000 plane strain shell elements

(continued)

Table 3 (continued)

First author, year	Margulies and Thibault [88]	(DeSantis) Klinich, [26]	Roth et al. [113, 114, 115]	Coats et al. [24]	Couper et al. [25]	Prange et al. [107]
Material law	Linear viscoelastic brain, linear elastic-plastic bone, springs for suture	Linear viscoelastic brain, linear elastic bone/suture/CSF/scalp	Linear viscoelastic brain, linear elastic bone (interpolated)/suture/CSF/scalp	Ogden brain, orthotropic linear elastic bone, linear elastic suture and scalp	Ogden with Maxwell for infinitesimal strains (various dissipation modes)	Ogden brain, rigid skull and falx
Validation	None	None	None	Skull fracture location as predicted by ultimate stress	None	None

shortcomings exist not only in the computational modeling field, but are also indicative of a general lack of experimental data.

10.3 Animal Head and Brain Models

In vivo TBI experiments animal surrogates are extensively used to study neurological responses, which cannot be investigated with cadavers or volunteers, as described in the introductory section to this chapter. Because there are many types of TBI in the human, no single published in vivo TBI experimental model can reproduce the entire spectrum of human TBI. To study individual brain injury types, different animal TBI experimental models have been developed. These experiments offer controlled and measurable external impact parameters which are uniquely suited to rigorous validation of FE simulations in multiple loading conditions, often an impediment to human FE model validation. Furthermore, the detailed brain internal injuries revealed through histological and/or imaging techniques can be compared against FE-predicted intracranial tissue response maps to study brain injury mechanisms as well as tolerance. In conjunction with human FE models, parallels can be drawn between human and animal injury, which may allow researchers to develop scaling laws to facilitate application of tolerance values from animal studies to human injury.

11 Rodent Brain FE Models

Among all the animals, rodents are the most frequently used animal in the laboratory for TBI experiments. Because of the minute nature of the rodent brain certain difficulties are encountered in the development of rodent FE brain models. Despite the extensive use of the rodent as a TBI experimental model, only five rodent FE brain models have been published to date, generally to investigate a specific experimental setup, limiting the ability to compare simulation predictions between different rat brain models based on what has been reported in the literature.

Shreiber et al. [129] developed 3-D FE rat brain model to study the mechanical threshold for blood-brain-barrier (BBB) injury. The model consisted of a homogeneous brain and a rigid skull which served as the boundary condition. In experimental studies, negative pressure pulses with magnitudes of 2, 3, and 4 psi (each at three different durations of 25, 50, and 100 ms) were applied to the exposed brain tissue to induce local brain deformation. The FE brain model calculated cortical displacement was then validated against experimentally measured brain surface deformation using a laser displacement transducer. The model-predicted maximum principal logarithmic strain, maximum principal stress, strain energy density, and von Mises stress were compared against the BBB injury

observed at specific locations within the brain. The authors reported that the maximum principal logarithmic strain was the best predictor with a strain value of 0.1888 for a 50% probability of BBB injury in rats.

Pena et al. [106] first attempted to characterize displacements, mean stress, and shear stress using a 2D FE brain model representing a single coronal section due to controlled cortical impact (CCI). Levchakov et al. [81] developed a 3D coarsely meshed FE model of a rat brain using tetrahedral elements to predict intracranial strain/stress for both neonate and mature rat brains in closed head CCI. Each of these two models assumed homogeneous material properties with no consideration given to the detailed anatomical organization of the brain. As such, these models are limited in their capability in predicting region-specific responses to TBI. The biofidelity of the above models are also questioned because neither has been validated against experimental data.

Mao et al. [85] developed a 3D FE rat brain model representing all essential anatomical features of a rat brain, including the olfactory bulb, cortex, hippocampus, thalamus, hypothalamus, corpus callosum, brainstem (midbrain, pons and medulla oblongata), cerebellum, lateral ventricle, third ventricle, fourth ventricle, internal capsule, external capsule and part of the spinal cord, based on histological studies of a rat brain [105]. The brain model consisted of 255,700 hexahedral elements with a typical spatial resolution 200 μm . The FE model was first validated against cortical tissue deformation measured during dynamic cortical deformation experiments conducted by Shreiber et al. [129]. The biomechanically validated rat brain model was then used to simulate four different series of CCI using unilateral craniotomy [19, 73, 127, 133]. Simulation results indicated that the peak maximum principal strain (MPS) with a threshold of 0.30 correlated with contusion volumes experimentally measured between 7 and 14 days post-injury. For predicting contusion measured at 24 h post-injury, 0.265 MPS is suggested [86]. To demonstrate the convergence of this rat brain model, Mao et al. [87] used five simplified 3D rat brain models with a spatial resolution of 1.6, 0.8, 0.4, 0.2, and 0.1 mm. Results demonstrated that continued decrease in element size resulted in less and less variation in the average MPS value. For example, the difference between the 1.6 and 0.8 mm spatial resolution models was 33.9% but the difference between the 0.2 and 0.1 mm resolution model was only 4.4% for the region close to impact area. Similarly, the differences for ventral region remote from impact were 42.7% between 1.6 and 0.8 mm spatial resolution model, and 1.1% between 0.2 and 0.1 mm resolution model. These results indicated that a model with 0.2 mm spatial resolution reasonably balanced between computational accuracy and efficiency at current stage.

Using the same rat brain model [85], Mao et al. [86, 87] proposed a new injury metrics: cumulative strain damage percentage measure (CSDPM). The CSDPM concept is based on the hypothesis that the element-level peak strain magnitude is related to the injury intensity within that element. In particular, the percentage of cell loss is found to be related to the magnitude of element strain. The difference between CSDPM and CSDM proposed by NHTSA researchers (see Sect. 2.1) is that CSDM counted the total volume of brain elements exceeding a certain

threshold strain value. In CSDPM, neuronal loss percentage was calculated for each brain element (~ 0.2 mm resolution for the FE rat brain model) first before the average percentage of cell loss for a region was determined. Equation 1 shows the proposed relationship between MPS and CSDPM [87]

$$\text{CSDPM} = \sum_{i=1}^N (1992 * \text{MPS} - 0.028) * [\text{volume ratio}(i)]$$

$$\text{Volume ratio}(i) = \frac{\text{volume of element}(i)}{\text{total brain volume}} \quad (1)$$

where i represents the brain element number and N is the total number of elements in the FE brain model.

The external impact parameters for the in vivo TBI models subjected to CCI tended to vary considerably among different laboratories, which make the comparison of research findings among different institutions very difficult. Mao et al. [87] adopted the design of experiments (DOE) method to investigate the effect of external impact parameters and the potential of using FE rat brain model previously developed by Mao et al. [85] to aid in the design of animal TBI model of desired injury intensity. A five-factor two-level fractional factorial DOE was performed. Results demonstrated that the impact depth was the leading factor affecting the predicted brain internal responses. Interestingly, impactor shape ranked as the second most important factor, surpassing impactor diameter and velocity, which were commonly reported in the literature as indicators of injury severity along with the impact depth. The differences in overall brain responses due to a unilateral craniotomy or bilateral craniotomies were small, but there were significant regional differences. The interaction effects of any two external parameters were found to be not significant. Such analysis demonstrates that FE rat brain model can be used to assist the engineering of better experimental TBI models in the future.

Shafieian et al. [128] developed a FE rat brain stem model to validate the assumption of force–displacement relationship during an in vitro indentation. The FE-predicted force–deflection curve agreed with the linear portion of the experimental results if the brainstem was modeled as a linear elastic material. At an impact depth of 0.5 mm, the FE model predicted a 20% effective strain at the ponto-medullary junction (PmJ) and a 38% effective strain at the pyramidal decussation (PDx). Quantification of axonal injuries yielded means of 1.7 ± 0.3 injured axons at PmJ, and 16.8 ± 1.1 at PDx per 100,000 μm^2 . The FE-predicted strains seemed to qualitatively match the trend of axonal injuries.

12 Primate Brain FE Models

Ward et al. [146] used both human and monkey finite element brain models developed by the same group [147] to predict intracranial pressure (ICP) in the human and monkey during blunt impact. The FE brain model was validated

against experimentally observed ICP data. By comparing ICP and brain injury in the form of contusion and hematoma/hemorrhage, Ward concluded that pressure above 234 kPa (34 psi) could induce severe brain injuries. However, due to the limited computational capabilities at that time, the brain meshes were relatively coarse. Tissue strains at both the coup and contre-coup sites were not investigated and their contributions to brain contusion remained unclear in the study.

In order to study the subdural hematoma injury mechanism, Lee et al. [80] developed a 2D rhesus monkey model to simulate the animal experiments designed and conducted by Abel et al. [1]. The brain was assumed to be an isotropic elastic material with a shear modulus of 80 kPa. The authors stated that this high shear modulus was selected to account for the absence of the dura, tentorium, and blood vessels. Structural damping was added in some simulations to remove the high frequency response components in the simulations. A no-slip boundary condition was assumed between the brain and skull. Because the authors were interested in establishing an injury threshold, which included both the peak linear and angular accelerations, they applied purely linear and purely angular loading to their model and calculated the brain deformation. The amount of linear loading required to generate the same deformation as a purely rotational loading was then determined to generate “equal deformation” lines on an angular versus tangential acceleration plot. From this point of view, a combined injury threshold was proposed.

13 Pig and Sheep Brain FE Models

In 1994, Zhou et al. developed three 2D finite element models representing three coronal sections of the porcine brain [162]. The models consisted of a three-layered skull, the dura, CSF, white matter, gray matter and ventricles. Model I was a section at the septal nuclei and anterior commissure level and contained 490 solid elements and 108 membrane elements. Model II was a section at the rostral-thalamic level and contained 644 solid elements and 130 membrane elements. Model III was a section at the caudal hippocampal level and contained 548 solid elements and 104 membrane elements. Plane strain conditions were assumed for all models. The input was the angular velocity time history used in the animal experiments performed at the University of Pennsylvania to determine the distribution of diffuse axonal injury (DAI) in porcine brain [112]. Regions of high shear stresses predicted by the model agreed qualitatively with experimental findings when the shear modulus of white matter was assumed to be 60% higher than that of gray matter. If the white and gray matter were assumed to possess the same properties, regions of DAI predicted by the model did not match those observed experimentally.

Miller’s study [93] focused on FE modeling approaches for the simulation of the relative motion between the skull and the cerebral cortex in miniature pigs.

They performed rotational acceleration tests along an axis normal to the axial plane (the plane perpendicular to the brainstem in a miniature pig), which, according to the authors, was equivalent to the coronal plane in the human. Diffuse axonal injury data from five experiments were used to validate their models which assumed that the skull and brain were either connected directly by a virtually incompressible low shear modulus material or by a frictional interface. The numerical responses of the two approaches were compared using the model across two-axial planes. Model I was partitioned through the dorsal part of the frontal, parietal and occipital lobes, while Model II was partitioned through the brain stem. The brain was assumed to be a Mooney–Rivlin hyperelastic material. When predicting the distribution of diffuse axonal injuries, results of their simulations demonstrated that the frictional interface was a better representation of the sub-arachnoid space than the virtually incompressible solid that had a low shear modulus. It was also found that the maximum principal nominal strain and von Mises stress were good predictors of axonal and macroscopic hemorrhagic cortical contusions, while negative pressure was a poor predictor for both forms of injury. A year later, Miller et al. [94] noted that most animal models provided only qualitative injury maps instead of quantitative ones for comparisons with FE model predictions, which could provide both temporal and spatial metrics for correlations with injury. They graded the severity of axonal injury from the animal experiments based on histological analyses. The two sectional models described in their 1998 paper [93] were separated into 20 regions for comparisons with experimentally observed graded injuries. They concluded that omitting the dura mater in the FE model of miniature pig could best approximate the graded experimental results they observed.

Anderson [5] developed a coarse-mesh 3D sheep brain model to simulate the blunt impact induced on the sheep head. He found that high von Mises stresses best correlated with their own axonal injury scores ($R^2 = 0.296$) among all parameters examined including strain and pressure. However, even in the best correlation case, the majority of the variation in axonal injury score was still unaccounted for. This seems to indicate numerical improvements of the coarse-mesh 3D brain model are required. Lastly, Zhu et al. [164] applied a 3D 3- to 5-day-old piglet brain model developed at the University of Pennsylvania to predict duration of unconsciousness. Using a published strain threshold developed previously with the same brain model, the length of unconscious time could be accurately predicted.

14 Other Animal Models

Ueno et al. [143] developed 3D FE ferret brain models that simulated the controlled cortical impacts performed at General Motors by Lighthall et al. [83]. The pressure predicted by the FE model compared favorably with experimental pressure data. The authors found that the pressure predicted by the FE model

propagated to the skull–brain boundary. High shear deformation was generated at the impact site and was similar to the contusion hemorrhage observed experimentally.


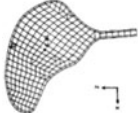
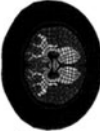



15 Summary of Animal FE Models

It can be seen that each of the animal brain FE models was developed for a specific purpose, and rarely were the computational models exercised fully. This makes it challenging to contrast the findings in any meaningful way. Instead, a brief summary of the aforementioned animal models is provided in Table 4 to illustrate how geometry, material laws, and validation compared. Except for the 3D rat brain model developed by Mao et al. [85] the rest of the animal models lacked detailed anatomical structures critical to the prediction of regional tissue responses for correlation with regional injury patterns and severities. Some of the models were not biomechanically validated and most of these animal FE models were developed to simulate a specific injury scenario without investigating other types of injury scenarios. Theoretically, a brain FE model with good biofidelity should be able to reasonably predict different types of TBI. In other words, it is better to evaluate a FE brain model for various types of TBI rather than for one specific condition so that its universal applicability and reliability can be assessed. FE model predictions need to be fully validated against multiple scenarios before they can be considered trustworthy and care must be taken when determining injury mechanisms and thresholds through comparisons of FE model predictions with experimentally obtained injury data.

16 Concluding Remarks

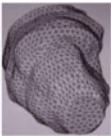





Any numerical model requires validation against multiple scenarios of experimental data before it can be used to predict model responses under conditions where experiments are difficult to conduct. In TBI impact biomechanics research, numerous researchers have emphasized the need for better characterizations of material laws and associated properties of brain and skull as they play important influential roles in simulation results. Additionally, numerical models developed thus far are in general under-validated due to lack of high fidelity data for model validation. For these reasons, it is recommended that head model developers should always conduct convergence study on the effect of mesh size before the simulated results are overused in predicting the injury outcomes. Limitations of models also need to be reported clearly. Nevertheless, a number of FE models have been developed and validated to a limited extent for advancing our understanding of head and brain biomechanics in hope to develop useful countermeasures to reduce the incidence of TBI.

Table 4 Summary of FE animal brain models

First author, Year	Ward et al. [146]	Lee et al. [80]	Zhou et al. [162]	Ueno et al. [143]	Miller et al. [93, 94]	Anderson [5]
Mesh						
Species	Monkey	Monkey	Pig	Ferret	Pig	Sheep
Solving software	NA	Nastran	PAM-CRASH	ABAQUS	ABAQUS	LS-DYNA
2D/3D	3D	2D	2D	3D	2D	3D
Geometry	Exact geometry	Mid-sagittal section	Atlas	Brain surface contour	T2 MRI	MRI, CT
Elements	NA	291 elements, 317 grid points	Model 1, 2, 3: 490, 644, 548 solid elements, and 108, 130, 104 membrane elements, respectively	1920 solid elements for brain, 883 shell elements for skull	NA	3936 solid elements, 1699 shell elements
Material law	Various elastic modulus and Poisson's ratio for brain	Brain as isotropic linear elastic material	Distinct gray and white matter, elastic material for brain, CSF, and skull	Elastic property for brain, rigid skull	Rigid skull, Mooney Rivlin for brain, distinct gray and white matter, elastic dura	Mooney-Rivlin for brain
Validation	Pressure	No	No	Pressure	No	No

(continued)

Table 4 (continued)

First author, Year	Zhu et al. [164]	Shreiber et al. [129]	Pena et al.[106]	Levchakov et al. [81]	Mao et al. [85, 86, 87]	Shafieian et al. [128]
Mesh						
Species	Pig	Rat	Rat	Rat	Rat	Rat brainstem
Solving software	ABAQUS	ABAQUS	FEMLab 2.0	Nastran	LS-DYNA	LS-DYNA
2D/3D	3D	3D	2D	3D	3D	3D
Geometry	MRI	Atlas	T2 MRI	Atlas	Atlas	Optical digitizer
Elements	66,445 Tetrahedral elements	36,664 solid elements	NA	About 30,000 tetrahedral elements	255,700 hexahedral elements	Hexahedral elements
Material law	Ogden material for brain	Modified hyperelastic material for brain, rigid skull	Elastic property for brain	Viscoelastic brain, elastic skull	Linear viscoelastic	Linear elastic
Validation	No	Cortical deformation	No	No	Cortical deformation	No

To overcome these difficulties is a monumental task which is probably why usable experimental data for validation are still lacking even after 70 years of TBI research. However, difficulties in conducting animal TBI research may not be as profound as using the human as research subjects. It is our belief that carefully designed animal experimental models with the aim of providing needed data for accurate material properties characterization and precise documentation of tissue-level impact responses will be the key to determining which techniques are most suitable for modeling the skull and brain tissues. Using these data, high resolution FE model can be developed to establish injury mechanisms and region-specific injury tolerances. If a number of high fidelity FE models representing a couple of small and large animals are successfully developed and rigorously validated, scaling laws and methodologies may be established to extrapolate animal responses to the human. The validated human head model will, in turn, be used to develop helmets or other countermeasures to mitigate the injury severity, reduce the number of TBI incidents, or even completely eliminate TBI.

Before this chapter is concluded, it is worth noting that none of the published numerical models addresses secondary brain injury, defined as a progressive cascade and evolution of primary injury or injury that is independent of the primary injury [20, 34, 43, 53]. This is because the passageway and progression from primary to secondary injury is mostly pathophysiological and therefore beyond the predictive capability of FE models at this time.

References

1. Abel, J.M., Gennarelli, T.A., Segawa, H.: Incidence and severity of cerebral concussion in the rhesus monkey following sagittal plane angular acceleration. In: 22nd Stapp Car Crash Conference. Ann Arbor, Michigan, USA (1978)
2. Al-Bsharat, A., Hardy, W.N., Yang, K.H., Khalil, T.B., King, A.I., Tashman, S.: Brain/skull relative displacement magnitude due to blunt head impact: new experimental data and model. In: 43rd Stapp Car Crash Conference, SAE Paper No. 99SC22. Society of Automotive Engineers, Warrendale (1999)
3. Alem, N.M., Simulation of head injury due to combined rotation and translation of the brain. In: Proceedings of the 18th Stapp Car Crash Conference, Ann Arbor, Michigan, USA, SAE 741192 (1974)
4. Allsop, D.L., Warner, C.Y., Wille, M.G., Scheider, D.C., Nahum, A.M.: Facial impact response—a comparison of the hybrid iii dummy and human cadaver. In: Proceedings of the 32nd Stapp Car Crash Conference, SAE Paper No. 881719. Society of Automotive Engineers, Warrendale (1988)
5. Anderson, R.W.: A study on the biomechanics of axonal injury. In: Road Accident Research Unit and the Department of Mechanical Engineering. The University of Adelaide (2000)
6. Bandak, F.A., Eppinger, R.H.: A three-dimensional finite element analysis of the human brain under combined rotational and translational accelerations. In: 38th Stapp Car Crash Conference, SAE 942215. Ft. Lauderdale, Florida, USA (1994)
7. Bandak, F.A.: On the mechanics of impact neurotrauma: a review and critical synthesis. *J. Neurotrauma* **12**(4), 635–649 (1995)

8. Bandak, F.A., Vander Vorst, M.J., Stuhmiller, L.M., Mlakar, P.F., Chilton, W.E., Stuhmiller, J.H.: An imaging-based computational and experimental study of skull fracture: finite element model development. *J. Neurotrauma* **12**(4), 679–688 (1995)
9. Bilston, L.E., Liu, Z., Phan-Thien, N.: Large strain behaviour of brain tissue in shear: some experimental data and differential constitutive model. *Biorheology* **38**(4), 335–345 (2001)
10. Brands, D.W., Bovendeerd, P.H., Peters, G.W., Wismans, J.S.: The large shear strain dynamic behaviour of in-vitro porcine brain tissue and a silicone gel model material. *Stapp Car Crash J.* **44**:249–260 (2000)
11. Brands, D.W.A., Bovendeerd, P.H.M., Wismans, J.S.H.M.: On the potential importance of non-linear viscoelastic material modelling for numerical prediction of brain tissue response: test and application. In: *Proceedings of the 46th Stapp Car Crash Conference*, pp. 103–121 (2002)
12. Chafi, M.S., Karami, G., Ziejewski, M.: An assessment of primary blast injury in human brains—a numerical simulation. In: *Proceedings of the 2007 ASME Summer Bioengineering Conference*, pp. 349–350 (2007a)
13. Chafi, M.S., Karami, G., Ziejewski, M.: Simulation of blast–head interactions to study traumatic brain injury. In: *Proceedings of the 2007 International Mechanical Engineering Congress and Exposition*, pp. 211–220 (2007b)
14. Chafi, M.S., Karami, G., Ziejewski, M.: Biomechanical assessment of brain dynamic responses due to blast pressure waves. *Ann Biomed Eng.* Epub (2009)
15. Chakrabarty, S.P., Hanson, F.B.: Distributed parameters deterministic model for treatment of brain tumors using galerkin finite element method. *Math. Biosci.* **219**(2), 129–141 (2009)
16. Chan, H.S.: Mathematical model for closed head impact. In: *Proceedings of the 18th Stapp Car Crash Conference*, SAE 741191. Ann Arbor, Michigan, USA (1974)
17. Chan, H.S., Liu, Y.K.: The symmetric response of a fluid-filled spherical shell—a mathematical simulation of a glancing blow to the head. *J. Biomech.* **7**, 43–59 (1974)
18. Chen, M., Mogul, D.J.: A structurally detailed finite element human head model for simulation of transcranial magnetic stimulation. *J. Neurosci. Methods* **179**(1), 111–120 (2009)
19. Chen, S., Pickard, J.D., Harris, N.G.: Time course of cellular pathology after controlled cortical impact injury. *Exp. Neurol.* **182**(1), 87–102 (2003)
20. Chen, Y.C., Smith, D.H., Meaney, D.F.: In vitro approaches for studying blast-induced traumatic brain injury. *J. Neurotrauma* **26**(6), 861–876 (2009)
21. Chu, C.S., Lin, M.S., Huang, H.M., Lee, M.C.: Finite element analysis of cerebral contusion. *J. Biomech.* **27**(2), 187–194 (1994)
22. Claessens, M., Sauren, F., Wismans, J.: Modeling of the human head under impact conditions: a parametric study. In: *Proceedings of the 41st Annual Stapp Car Crash Conference*, SAE 973338. Lake Buena Vista, Florida, USA (1997)
23. Cloots, R.J., Gervaise, H.M., van Dommelen, J.A., Geers, M.G.: Biomechanics of traumatic brain injury: influences of the morphologic heterogeneities of the cerebral cortex. *Ann. Biomed. Eng.* **36**(7), 1203–1215 (2008)
24. Coats, B., Margulies, S.S., Ji, S.: Parametric study of head impact in the infant. *Stapp. Car Crash J.* **51**, 1–15 (2007)
25. Couper, Z., Albermani, F.: Infant brain subjected to oscillatory loading: material differentiation, properties, and interface conditions. *Biomech. Model. Mechanobiol.* **7**(2), 105–125 (2008)
26. Desantis-Klinich, K.D., Hulbert, G., Schneider, L.W.: Estimating infant head injury criteria and impact response using crash reconstruction and finite element modeling. *Stapp Car Crash J.* **46**, 165–194 (2002)
27. Dimasi, F., Eppinger, R.H., Gabler, H.C., Marcus, J.: Simulated head impacts with upper interior structures using rigid and anatomic brain models. In: R. Strombotne (ed.) *Auto and Traffic Safety*, vol. 1, no. 1. National Highway Traffic Safety Publication, Washington, D.C. USA (1991)

28. DiMasi, F.P., Eppinger, R.H., Bandak, F.A.: Computational analysis of head impact response under car crash loadings. In: Proceedings of the 39th Stapp Car Crash Conference, SAE 952718, San Diego, CA, USA (1995)
29. Engin, A.E., Liu, Y.K.: Axisymmetric response of a fluid-filled spherical shell in free vibrations. *J. Biomech.* **3**(1), 11–22 (1970)
30. Eppinger, R., Kleinberger, M., Morgan, R., Khaewpong, N., Bandak, F.A., Haffner, M.: Advanced injury criteria and crash test evaluation techniques. In: Proceedings of the NHTSA 14th International Technical Conference on Experimental Safety Vehicles, Paper no. 90-S1-O-11. Munich, Germany (1994)
31. Fan, W.R.S.: Internal head injury assessment. In: Proceedings of the 15th Stapp Car Crash Conference, SAE 710870. San Diego, CA, USA (1971)
32. Finkel, M.F.: The neurological consequences of explosives. *J. Neurol. Sci.* **249**, 63–67 (2006)
33. Finkelstein, E., Corso, P., Miller, T., and Associates.: The Incidence and Economic Burden of Injuries in the United States. Oxford University Press, New York (2006)
34. Fitch, M.T., Doller, C., Combs, C.K., Landreth, G.E., Silver, J.: Cellular and molecular mechanisms of glial scarring and progressive cavitation: in vivo and in vitro analysis of inflammation-induced secondary injury after cns trauma. *J. Neurosci.* **19**(19), 8182–8198 (1999)
35. Franklyn, M., Fildes, B., Zhang, L., Yang, K., Sparke, L.: Analysis of finite element models for head injury investigation: reconstruction of four real-world impacts. *Stapp Car Crash J.* **50** (2005)
36. Franklyn, M., Peiris, S., Huber, C., Yang, K.H.: Pediatric material properties: a review of human child and animal surrogates. *Crit. Rev. Biomed. Eng.* **35**(3–4), 197–342 (2007)
37. Fredriksson, R., Zhang, L., Boström, O., Yang, K.H.: Influence of Impact Speed on Head and Brain Injury Outcome in Vulnerable Road User Impacts to the Car Hood. *Stapp Car Crash J.* **51**, 155–167 (2007)
38. Galford, J.E., McElhaney, J.H.: A viscoelastic study of scalp, brain, and dura. *J. Biomech.* **3**(2), 211–221 (1970)
39. Gao, C., Tay, H., Nowinski, F., Wieslaw, L.: A finite element method based deformable brain atlas suited for surgery simulation. In: Conf Proc IEEE Eng Med Biol Soc. vol. 4, pp. 4337–4340 (2005)
40. Gao, C.P., Ang, B.T.: Biomechanical modeling of decompressive craniectomy in traumatic brain injury. *Acta Neurochir. Suppl.* **102**, 279–282 (2008)
41. Goldsmith, W.: The physical processes producing head injury. In: Proceedings of the Head Injury Conference, pp. 350–382. Lippincott, PA (1966)
42. Gondusky, J.S., Reiter, M.P.: Protecting military convoys in Iraq: an examination of battle injuries sustained by a mechanized battalion during Operation Iraqi Freedom II. *Mil. Med.* **170**(6), 546–549 (2005)
43. Greve, M.W., Zink, B.J.: Pathophysiology of traumatic brain injury. *Mt Sinai J. Med.* **76**(2), 97–104 (2009)
44. Hagemann, A., Rohr, K., Stiehl, H.S.: Coupling of fluid and elastic models for biomechanical simulations of brain deformations using FEM. *Med. Image Anal.* **6**(4), 375–388 (2002)
45. Hardy, C.H., Marcal, P.V.: Elastic Analysis of a Skull. Technical Report No. 8, Office of Naval Research, Contract No. N00014-67-A-0191–0007, Div. Eng, Brown University (1971)
46. Hardy, W.N., Foster, C.D., Mason, M.J., Yang, K.H., King, A.I., Tashman, S.: Investigation of head injury mechanisms using neutral density technology and high-speed biplanar X-ray. *Stapp Car Crash J.* **45**, 337–368 (2001)
47. Hardy, W.N., Mason, M.J., Foster, C.D., Shah, C.S., Kopacz, J.M., Yang, K.H., King, A.I., Bishop, J., Bey, M., Anderst, W., Tashman, S.: A study of the response of the human cadaver head to impact. *Stapp Car Crash J.* **51**, 17–80 (2007)

48. Ho, J., Kleiven, S.: Dynamic response of the brain with vasculature: a three-dimensional computational study. *J. Biomech.* **40**(13), 3006–3012 (2007)
49. Ho, J., Kleiven, S.: Can sulci protect the brain from traumatic injury? *J. Biomech.* **42**(13), 2074–2080 (2009)
50. Hodgson, V.R., Gurdjian, E.S., Thomas, L.M.: Development of a model for the study of head injury during impact tests. In: *Proceedings of the 11th Stapp Car Crash Conference*, SAE 670923. Anaheim, CA, USA (1967)
51. Hodgson, V.R., Patrick, L.M.: (1968) Dynamic response of the human cadaver head compared to a simple mathematical model. In: *Proceedings of the 12th Stapp Car Crash Conference*, SAE 680784. Detroit, Michigan, USA
52. Horgan, T.J., Gilchrist, M.D.: The creation of three-dimensional finite element models for simulating head impact biomechanics. *Int. J. Crashworthiness* **8**(4), 353–366 (2003)
53. Holmberg, P., Liljequist, S., Wagner, A.: Secondary brain injuries in thalamus and hippocampus after focal ischemia caused by mild, transient extradural compression of the somatosensory cortex in the rat. *Curr. Neurovasc. Res.* **6**(1), 1–11 (2009)
54. Hosey, R.R., Liu, Y.K.: A homeomorphic finite element model of the human head and neck. In: Gallagher, P.H., Simon, B.R., Johnson, T.C., Gross, J.F. (eds.) *Finite Element in Biomechanics*, pp. 379–401. Wiley, New York (1982)
55. Hu, J., Jin, X., Lee, J.B., Zhang, L., Chaudhary, V., Guthikonda, M., Yang, K.H., King, A.I.: Intraoperative brain shift prediction using a 3D inhomogeneous patient-specific finite element model. *J. Neurosurg.* **106**(1), 164–169 (2007)
56. Huang, H.M., Lee, M.C., Lee, S.Y., Chiu, W.T., Pan, L.C., Chen, C.T.: Finite element analysis of brain contusion: an indirect impact study. *Med. Biol. Eng. Comput.* **38**(3), 253–259 (2000)
57. Jin, X., Lee, J.B., Leung, L.Y., Zhang, L., Yang, K.H., King, A.I.: Biomechanical response of the bovine pia-arachnoid complex to tensile loading at varying strain-rates. *Stapp Car Crash J.* **50**, 637–649 (2006)
58. Jin, X., Ma, C., Zhang, L., Yang, K.H., King, A.I., Dong, G., Zhang, J.: Biomechanical response of the bovine pia-arachnoid complex to normal traction loading at varying strain rates. *Stapp Car Crash J.* **51**, 115–126 (2007)
59. Jin, X., Yang, K.H., King, A.I.: Mechanical properties of bovine pia-arachnoid complex in shear. *J. Biomech.* (2010). [Epub ahead of print] 2010 Nov 17
60. Johnson, E.A., Young, P.G.: On the use of a patient-specific rapid-prototyped model to simulate the response of the human head to impact and comparison with analytical and finite element models. *J. Biomech.* **38**(1), 39–45 (2005)
61. Kang, H., Willinger, R., Diaw, R.M., Chinn, B.P.: Validation of a 3D anatomic human head model and replication of head impact in motorcycle accident by finite element modeling. In: *41st Stapp Car Crash Conference*, SAE 973339. Lake Buena Vista, Florida, USA (1997)
62. Khalil, T.B., Goldsmith, W., Sackman, J.L.: Impact on a model head-helmet system. *Int. J. Mech. Sci.* **16**, 609–625 (1974)
63. Khalil, T.B., Hubbard, R.P.: Parametric study of head response by finite element modeling. *J. Biomech.* **10**(2), 119–132 (1977)
64. Khalil, T.B., Viano, D.C.: Critical issues in finite element modeling of head impact. In: *Proceedings of the 26th Stapp Car Crash Conference*, Ann Arbor, Michigan, USA, SAE 821150 (1982)
65. Kimpara, H., Nakahira, Y., Iwamoto, M., Miki, K., Ichihara, K., Kawano, S., Taguchi, T.: Investigation of anteroposterior head-neck responses during severe frontal impacts using a brain-spinal cord complex FE model. *Stapp Car Crash J.* **50**, 509–544 (2006)
66. King, A.I., Chou, C.C.: Mathematical modeling, simulation and experimental testing of biomechanical system crash response. *J. Biomech.* **9**, 301–317 (1976)
67. King, A.I., Yang, K.H., Hardy, W.N., Al-Bsharat, A.S., Deng, B., Begeman, P.C., Tashman, S.: Challenging problems and opportunities in impact biomechanics. In: *Proceedings of the 1999 Bioengineering Conference*, ASME, pp. 269–270 (1999)

68. Kleiven, S., von Holst, H.: Consequences of head size following trauma to the human head. *J. Biomech.* **35**(2), 153–160 (2002)
69. Kleiven, S., Hardy, W.N.: Correlation of an FE model of the human head with local brain motion—consequences for injury prediction. *Stapp Car Crash J.* **46**, 123–144 (2002)
70. Kleiven, S.: Influence of impact direction on the human head in prediction of subdural hematoma. *J. Neurotrauma* **20**(4), 365–379 (2003)
71. Kleiven, S.: Evaluation of head injury criteria using a finite element model validated against experiments on localized brain motion, intracerebral acceleration, and intracranial pressure. *Int. J. Crashworthiness* **11**(1), 65–79 (2006)
72. Kleiven, S.: Predictors for traumatic brain injuries evaluated through accident reconstructions. *Stapp Car Crash J.* **51**, 81–114 (2007)
73. Kochanek, P.M., Marion, D.W., Zhang, W., Schiding, J.K., White, M., Palmer, A.M., Clark, R.S., O'Malley, M.E., Styren, S.D., Ho, C., DeKosky, S.T.: Severe controlled cortical impact in rats: assessment of cerebral edema, blood flow, and contusion volume. *J. Neurotrauma* **12**(6), 1015–1025 (1995)
74. Krabbel, G., Appel, H.: Development of a finite element model of the human skull. *J. Neurotrauma* **12**(4), 735–742 (1995)
75. Kuijpers, A.H., Claessens, M.H., Sauren, A.A.: The influence of different boundary conditions on the response of the head to impact: a two-dimensional finite element study. *J. Neurotrauma* **12**(4), 715–724 (1995)
76. Kumaresan, S., Radhakrishnan, S.: Importance of partitioning membranes of the brain and the influence of the neck in head injury modelling. *Med. Biol. Eng. Comput.* **34**(1), 27–32 (1996)
77. Kurosawa, Y., Kato, K., Takahashi, T., Kubo, M., Uzuka, T., Fujii, Y., Takahashi, H.: 3-D finite element analysis on brain injury mechanism. In: *Conf Proc IEEE Eng Med Biol Soc.*, 4090-3 (2008)
78. Kurtz, S.M., Thibault, K.L., et al.: Finite element analysis of the deformation of the human infant head under impact conditions. In: *The Proceedings of the 8th Injury Prevention through Biomechanics Symposium*. Wayne State University, Detroit, Michigan (1998)
79. Langlois, J.A., Rutland-Brown, W., Thomas, K.E.: *Traumatic brain injury in the United States: Emergency Department Visits, Hospitalizations, and Deaths*. Centers for Disease Control and Prevention, National Center for Injury Prevention and Control (2006)
80. Lee, M.C., Melvin, J.W., Ueno, K.: Finite element analysis of traumatic subdural hematoma. In: *31st Stapp Car Crash Conference*, SAE 872201. New Orleans, LA, USA (1987)
81. Levchakov, A., Linder-Ganz, E., Raghupathi, R., Margulies, S.S., Gefen, A.: Computational studies of strain exposures in neonate and mature rat brains during closed head impact. *J. Neurotrauma* **23**(10), 1570–1580 (2006)
82. Li, J., Zhang, J., Yoganandan, N., Pintar, F., Gennarelli, T.: Regional brain strains and role of falx in lateral impact-induced head rotational acceleration. *Biomed. Sci. Instrum.* **43**, 24–29 (2007)
83. Lighthall, J.W., Melvin, J.W., Ueno, K.: Toward a biomechanical criterion for functional brain injury. In: *Proceedings of 12th International Technical Conference on Experimental Safety Vehicles*, pp. 627–633 (1989)
84. Ling, G., Bandak, F., Armonda, R., Grant, G., Ecklund, J.: Explosive blast neurotrauma. *J. Neurotrauma* **2007**(26), 815–825 (2009)
85. Mao, H., Zhang, L., Yang, K.H., King, A.I.: Application of a finite element model of the brain to study traumatic brain injury mechanisms in the rat. *Stapp Car Crash J.* **50**, 583–600 (2006)
86. Mao, H., Jin, X., Zhang, L., Yang, K.H., Igarashi, T., Noble, L.J., King, A.I.: Finite element analysis of controlled cortical impact induced cell loss. *J. Neurotrauma* **27**, 877–888 (2010)
87. Mao, H., Yang, K.H., King, A.I., Yang, K.: Computational neurotrauma—design, simulation, and analysis of controlled cortical impact model. *Biomech Model Mechanobiol* (2010). doi:[10.1007/s10237-010-0212-z](https://doi.org/10.1007/s10237-010-0212-z)

88. Margulies, S.S., Thibault, K.L.: Infant skull and suture properties: measurements and implications for mechanisms of pediatric brain injury. *J. Biomech. Eng.* **122**(4), 364–371 (2000)
89. Marjoux, D., Baumgartner, D., Deck, C., Willinger, R.: Head injury prediction capability of the HIC, HIP, SIMon and ULP criteria. *Accid. Anal. Prev.* **40**(3), 1135–1148 (2008)
90. Martinez, J.L.: Headrest and seat back proposals designed to eliminate head and neck injuries. In: *Proceedings of the 12th Stapp Car Crash Conference*, Detroit, Michigan, USA, SAE 680775 (1968)
91. Merchant, H.C., Crispino, A.J.: A dynamic analysis of an elastic model of the human head. *J. Biomech.* **7**(3), 295–301 (1974)
92. Meyer, R., Kohler, J., Homburg, A.: *Explosives*, 5th edition. Wiley-VCH, Weinheim, Germany (2002)
93. Miller, R.T., Margulies, S.S., Leoni, M., Nonaka, M., Chen, X., Smith, D.H., Meaney, D.F.: Finite element modeling approaches for predicting injury in an experimental model of severe diffuse axonal injury. 42nd Stapp Car Crash Conference, SAE 983154. Tempe, AZ, USA (1998)
94. Miller, R.T., Smith, D.H., Chen, X., Xu, B., Leoni, M., Nonaka, M., Meaney, D.F.: Comparing experimental data to traumatic brain injury finite element models. In: 43rd Stapp Car Crash Conference, SAE 99SC20. San Diego, CA, USA (1999)
95. Moss, W., King, M.J., Blackman, E.C.: Skull flexure form blast waves: a new mechanism for brain injury with implications for helmet design. *J. Acoust. Soc. Am.* **125**(4), 2650–2665 (2009)
96. Moore, D.F., Jerusalem, A., Nyein, M., Noels, L., Jaffee, M.S., Radovitzky, R.A.: Computational biology—modeling of primary blast effects on the central nervous system. *Neuroimage* **47**(Suppl 2), 10–20 (2009)
97. Nahum, A.M., Smith, R., Ward, C.C.: Intracranial pressure dynamics during head impact. In: *Proceedings of the 21st Stapp Car Crash Conference*, SAE Paper No. 770922. Society of Automotive Engineers, Warrendale, PA (1977)
98. Nahum, A.M., Smith, R.W., Raasch, F.D., Ward, C., 1979. Intracranial pressure relationships in the protected and unprotected head. In: *Proceedings of the 23rd Stapp Car Crash Conference*, SAE 791024. San Diego, California, USA
99. Nahum, A., Ward, C., Raasch, E., Adams, S., Schneider, D.: Experimental studies of side impact to the human head. In: *Proceedings of the 24th Stapp Car Crash Conference*, Troy, Michigan, USA, SAE 801301 (1980)
100. Nahum, A.M., Ward, C., Schneider, D., Raasch, F., Adams, S.: A study of impacts to the lateral protected and unprotected head. In: 25th Stapp Car Crash Conference, San Francisco, CA, SAE Paper No. 811006 (1981)
101. Newman, J.A., Shewchenko, N., Welbourne, E.: A proposed new biomechanical head injury assessment function—the maximum power index. In: 44th Stapp Car Crash Conf. SAE 2000-01-SC16 (2000)
102. Nyquist, G.W., Cavanaugh, J.M., Goldberg, S.J., King, A.I.: Facial impact tolerance and response. In: *Proceedings of the 30th Stapp Car Crash Conference*, SAE Paper No. 861896. Society of Automotive Engineers, Warrendale, PA (1986)
103. Okie, S.: Traumatic brain injury in the war zone. *N. Engl. J. Med.* **352**(20), 2043–2047 (2005)
104. Pintar, F.A., Yoganandan, N., Voo, L., Cusick, J.F., Maiman, D.J., Sances, A. Jr.: Dynamic characteristics of the human cervical spine. In: *Proceedings of the 39th Stapp Car Crash Conference*, San Diego, CA Nov 8–10, SAE 952722 (1995)
105. Paxinos, G., Watson, C.: *The Rat Brain in Stereotaxic Coordinates*. Elsevier, San Diego (2005)
106. Pena, A., Pickard, J.D., Stiller, D., Harris, N.G., Schuhmann, M.U.: Brain tissue biomechanics in cortical contusion injury: a finite element analysis. *Acta Neurochir. Suppl.* **95**, 333–336 (2005)

107. Prange, M.T., Kiralyfalvi, G., Margulies, S.S.: Pediatric rotational inertial brain injury: the relative influence of brain size and mechanical properties. Stapp Car Crash Conference, SAE 99SC23. San Diego, California, USA (1999)
108. Prange, M.T., Meaney, D.F., Margulies, S.S.: Defining brain mechanical properties: effects of region, direction, and species. In: Proceedings of the 44th Stapp Car Crash Conference, Atlanta, Georgia, USA, SAE 2000-01-SC15 44:205–213 (2000)
109. Prange, M.T., Margulies, S.S.: Regional, directional, and age-dependent properties of the brain undergoing large deformation. *J. Biomech. Eng.* **124**(2), 244–252 (2002)
110. Raul, J.S., Baumgartner, D., Willinger, R., Ludes, B.: Finite element modelling of human head injuries caused by a fall. *Int. J. Leg. Med.* **120**(4), 212–218 (2006)
111. Raul, J.S., Deck, C., Willinger, R., Ludes, B.: Finite-element models of the human head and their applications in forensic practice. *Int. J. Leg. Med.* **122**(5), 359–366 (2008)
112. Ross, D.T., Meaney, D.F., Sabol, M.K., Smith, D.H., Gennarelli, T.A.: Distribution of forebrain diffuse axonal injury following inertial closed head injury in miniature swine. *Exp. Neurol.* **126**(2), 291–299 (1994)
113. Roth, S., Raul, J.S., Ludes, B., Willinger, R.: Finite element analysis of impact and shaking inflicted to a child. *Int. J. Leg. Med.* **121**(3), 223–228 (2007)
114. Roth, S., Raul, J.S., Willinger, R.: Biofidelic child head FE model to simulate real world trauma. *Comput. Methods Programs Biomed.* **90**(3), 262–274 (2008)
115. Roth, S., Vappou, J., Raul, J.S., Willinger, R.: Child head injury criteria investigation through numerical simulation of real world trauma. *Comput. Methods Programs Biomed.* **93**(1), 32–45 (2009)
116. Rousseau, P., Hoshizaki, T.B., Gilchrist, M.D., Post, A.: Estimating the influence of neckform compliance on brain tissue strain during helmeted impact. *Stapp Car Crash J.* **54**, 37–48 (2010)
117. Ruan, J.S., Khalil, T., King, A.I.: Human head dynamic response to side impact by finite element modeling. *J. Biomech. Eng.* **113**(3), 276–283 (1991)
118. Ruan, J.S., Khalil, T., King, A.I.: Finite element modeling of direct head impact. 37th Stapp Conference proceedings, SAE 933114. San Antonio, TX (1993)
119. Ruan, J.S., Khalil, T., King, A.I.: Dynamic response of the human head to impact by three-dimensional finite element analysis. *J. Biomech. Eng.* **116**(1), 44–50 (1994)
120. Ruan, J.S., Prasad, P.: Head injury potential assessment in frontal impacts by mathematical modeling. In: Proceedings of the 38th Stapp Car Crash Conference, SAE 942212. Ft. Lauderdale, Florida, USA (1994)
121. Ruan, J.S., Prasad, P.: Coupling of a finite element human head model with a lumped parameter hybrid iii dummy model: preliminary results. *J. Neurotrauma* **12**(4), 725–734 (1995)
122. Ruan, J., Prasad, P.: The effects of skull thickness variations on human head dynamic impact responses. *Stapp Car Crash J.* **45**, 395–414 (2001)
123. Ruan, J.S., Prasad, P.: Comments: on the consequences of head size following impact to the human head. *J. Biomech.* **39**(2): 383–385; author reply 385–387 (2006)
124. Saberli, H., Seddighi, A.S., Farmanzad, F.: Finite element analysis of an elastic model of the brain: distortion due to acute epidural hematoma—the role of the intra-ventricular pressure gradient. *Comput Aided Surg.* **12**(2), 131–136 (2007)
125. Saczalski, K.J., Richardson, E.Q.: Nonlinear numerical prediction of human head/helmet crash impact response. *Aviat. Space Environ. Med.* **49**(1 Pt. 2):114–119 (1978)
126. Sarron, J.C., Caillou, J.P., Da Cunha, J., Allain, J.C., Tramecon, A.: Consequences of nonpenetrating projectile impact on a protected head: study of rear effects of protections. *J. Trauma* **49**(5), 923–929 (2000)
127. Scheff, S.W., Baldwin, S.A., Brown, R.W., Kraemer, P.J.: Morris water maze deficits in rats following traumatic brain injury: lateral controlled cortical impact. *J. Neurotrauma* **14**(9), 615–627 (1997)
128. Shafieian, M., Darvish, K.K., Stone, J.R.: Changes to the viscoelastic properties of brain tissue after traumatic axonal injury. *J. Biomech.* **42**(13), 2136–2142 (2009)

129. Shreiber, D.I., Bain, A.C., Meaney, D.F.: In vivo thresholds for mechanical injury to the blood-brain barrier. In: 41th Stapp Car Crash Conference, SAE 973335. Lake Buena Vista, Florida, USA (1997)
130. Shugar, T.A.: Transient structural response of the linear skull-brain system. Proceedings of the 19th Stapp Car Crash Conference, SAE 751161. San Diego, California, USA (1975)
131. Slattenschek, A., Tauffkirchen, W., Benedikter, G.: Quantification of internal head injury by means of the phantom head and the impact assessment methods. In: Proceedings of the 15th Stapp Car Crash Conference, SAE 710879. San Diego, California, USA (1971)
132. Soza, G., Grosso, R., Labsik, U., Nimsky, C., Fahlbusch, R., Greiner, G., Hastreiter, P.: Fast and adaptive finite element approach for modeling brain shift. *Comput. Aided Surg.* **8**(5), 241–246 (2003)
133. Sutton, R.L., Lescaudron, L., Stein, D.G.: Unilateral cortical contusion injury in the rat: vascular disruption and temporal development of cortical necrosis. *J. Neurotrauma* **10**(2), 135–149 (1993)
134. Takhounts, E.G., Eppinger, R.H., Campbell, J.Q., Tannous, R.E., Power, E.D., Shook, L.S.: On the development of the Simon finite element head model. *Stapp Car Crash J.* **47**, 107–133 (2003)
135. Takhounts, E.G., Ridella, S.A., Hasija, V., Tannous, R.E., Campbell, J.Q., Malone, D., Danelson, K., Stitzel, J., Rowson, S., Duma, S.: Investigation of traumatic brain injuries using the next generation of simulated injury monitor (simon) finite element head model. *Stapp Car Crash J.* **52**, 1–31 (2008)
136. Takizawa, H., Sugiura, K., Baba, M., Miller, J.D.: Analysis of intracerebral hematoma shapes by numerical computer simulation using the finite element method. *Neurol Med Chir (Tokyo)* **34**(2), 65–69 (1994)
137. Taylor, P.A., Ford, C.C.: Simulation of blast-induced early-time intracranial wave physics leading to traumatic brain injury. *J. Biomech. Eng.* **131**(6), 061007 (2009)
138. Thibault, K.T., Kurtz, S.M., Margulies, S.S.: Effect of the age-dependent properties of the braincase on the response of the infant brain to impact. *BED Adv. Bioeng.*, In Proceedings for the Winter Annual Meeting of the ASME (1997)
139. Thurman, D.J., Alverson, C., Browne, D.: Traumatic brain injury in the United States: a report to congress. Centers for Disease Control and Prevention, National Center for Injury Prevention and Control (2000)
140. Trosseille, X., Tarriere, C., Lavaste, F., Guillon, F., Domont, A.: Development of a FEM of the human head according to a specific test protocol. In: Proceedings of 30th Stapp Car Crash Conference, SAE 922527, pp. 235–253 (1992)
141. Thunnissen, J.G.M., Wismans, J.S.H.M., Ewing, C.L., Thomas, D.J.: Human volunteer head-neck response in frontal flexion: a new analysis. In: Proceedings of the 39th Stapp Car Crash Conference, SAE 952721 (1995)
142. Turquier, F., Trosseille, X., Lavaste, F., Tarriere, C., Dômont, A., Kang, H.S., Willinger, R.: Validation study of a 3D finite element head model against experimental data. In: 40th Stapp Car Crash Conference, SAE 962431. Albuquerque, New Mexico, USA (1996)
143. Ueno, K., Melvin, J.W., Li, L., Lighthall, J.W.: Development of tissue level brain injury criteria by finite element analysis. *J. Neurotrauma* **12**(4), 695–706 (1995)
144. Viano, D.C., Casson, I.R., Pellman, E.J., Zhang, L., King, A.I., Yang, K.H.: Concussion in professional football: brain responses by finite element analysis: Part 9. *Neurosurgery* **57**(5), 891–916; discussion 891–916 (2005)
145. Ward, C.: Finite element models of the head and their use in brain injury research. In: Proceedings of the 26th Stapp Car Crash Conference, SAE 821154. Ann Arbor, Michigan, USA (1982)
146. Ward, C.C., Chan, M., Nahum, A.M.: Intracranial pressure—a brain injury criterion. In: 24th Stapp Car Crash Conference, SAE 801304, Troy, Michigan, USA (1980)
147. Ward, C.C., Nikravesh, P.E., Thompson, R.B.: Biodynamic finite element models used in brain injury research. *Aviat Space Environ. Med.* **49**(1 Pt. 2), 136–142 (1978)

148. Ward, C., Thompson, R.B.: The development of a detailed finite element brain model. In 19th Stapp Car Crash Conference, SAE 751163. San Diego, CA, USA (1975)
149. Willinger, C.M., Kopp, D., Cesari, D.: New concept of contrecoup lesions mechanism: modal analysis of a finite element head model, pp. 283–297. IRCOBI Verona, Italy (1992)
150. Willinger, R., Taleb, L., Kopp, C.M.: Modal and temporal analysis of head mathematical models. *J. Neurotrauma* **12**(4), 743–754 (1995)
151. Willinger, R., Taled, L., Pradoura, P.: Head biomechanics from the finite element model to the physical model, pp. 245–260. IRCOBI, Brunnen, Switzerland (1995)
152. Willinger, R., Kang, H.S., Diaw, B.: Three-dimensional human head finite-element model validation against two experimental impacts. *Ann. Biomed. Eng.* **27**(3), 403–410 (1999)
153. Wittek, A., Kikinis, R., Warfield, S.K., Miller, K.: Brain shift computation using a fully nonlinear biomechanical model. *Medical Image Computing and Computer-Assisted Intervention—MICCAI* **8**(Pt 2), 583–590 (2005)
154. Wittek, A., Dutta-Roy, T., Taylor, Z., Horton, A., Washio, T., Chinzei, K., Miller, K.: Subject-specific non-linear biomechanical model of needle insertion into brain. *Comput. Methods Biomech. Biomed. Eng.* **11**(2), 135–146 (2008)
155. Xu, W., Yang, J.: Development and validation of head finite element model for traffic injury analysis. *Sheng Wu Yi Xue Gong Cheng Xue Za Zhi.* **25**(3), 556–561 (2008)
156. Yoganandan, N., Li, J., Zhang, J., Pintar, F.A., Gennarelli, T.A.: Influence of angular acceleration–deceleration pulse shapes on regional brain strains. *J. Biomech.* **41**(10), 2253–2262 (2008)
157. Zhang, J., Yoganandan, N., Pintar, F.A., Gennarelli, T.A.: Brain strains in vehicle impact tests. *Annu. Proc. Assoc. Adv. Automot. Med.* **50**, 1–12 (2006)
158. Zhang, J., Yoganandan, N., Pintar, F.A., Gennarelli, T.A., Shender, B.S.: A finite element study of blast traumatic brain injury—biomed 2009. *Biomed. Sci. Instrum.* **45**, 119–124 (2009)
159. Zhang, L., Bae, J., Hardy, W.N., Monson, K.L., Manley, G.T., Goldsmith, W., Yang, K.H., King, A.I.: Computational study of the contribution of the vasculature on the dynamic response of the brain. *Stapp Car Crash J.* **46**, 145–164 (2002)
160. Zhang, L., Yang, K.H., King, A.I.: Comparison of brain responses between frontal and lateral impacts by finite element modeling. *J. Neurotrauma* **18**(1), 21–30 (2001a)
161. Zhang, L., Yang, K.H., Dwarampudi, R., Omori, K., Li, T., Chang, K., Hardy, W.N., Khalil, T.B., King, A.I.: Recent advances in brain injury research: a new human head model development and validation. *Stapp Car Crash J.* **45**, 369–394 (2001b)
162. Zhou, C., Khalil, T.B., King, A.I.: Shear stress distribution in the porcine brain due to rotational impact. In: 38th Stapp Car Crash Conference, SAE 942214. Ft. Lauderdale, Florida, USA (1994)
163. Zhou, C., Khalil, T.B., King, A.I.: A new model comparing impact responses of the homogeneous and inhomogeneous human brain. In: Proceedings of the 39th Stapp Car Crash Conference, SAE Paper No. 952714. Society of Automotive Engineers, Warrendale, PA (1995)
164. Zhu, Q., Prange, M., Margulies, S.: Predicting unconsciousness from a pediatric brain injury threshold. *Dev. Neurosci.* **28**(4–5), 388–395 (2006)
165. Zhu, F., Mao, H., Dal Cengio Leonardi, A., Wagner, C., Chou, C., Jin, X., Bir, C., VandeVord, P., Yang, K.H., King, A.I.: Development of an FE model of the rat head subjected to air shock loading. *Stapp Car Crash J.* **54**, 211–225 (2010)
166. Zong, Z., Lee, H.P., Lu, C.: A three-dimensional human head finite element model and power flow in a human head subject to impact loading. *J. Biomech.* **39**(2), 284–292 (2006)
167. Zoroya, G.: Key Iraq wound: Brain Trauma, in USA Today (2005)